HAZE IN THE MARS ATMOSPHERE AS REVEALED BY THE MARINER IV TELEVISION DATA

August 20, 1968

Bellcomm, Inc.

BELLCOMM, INC.

TR-68-710-6

HAZE IN THE MARS ATMOSPHERE AS REVEALED BY THE MARINER IV TELEVISION DATA

August 20, 1968

P. L. Chandeysson
E. N. Shipley
W. B. Thompson

Work performed for Manned Space Flight, National Aeronautics and Space Administration under Contract NASW-417.

TABLE OF CONTENTS

ABSTRACT

A photometric model for Mars has been developed which explains all the relevant features of the Mariner IV television data. The dominant feature of the model is a haze component in the atmosphere which substantially affects the overall scene brightness. The model can be used to subtract the haze effect from available pictures or to compute scene brightness in geometries different from those of Mariner IV.

HAZE IN THE MARS ATMOSPHERE AS REVEALED BY THE MARINER IV TELEVISION DATA

I. Introduction

Adequate planning of photographic experiments for future space missions to Mars requires an understanding of the basic light scattering, absorbing, and reflecting properties of the planet, including its atmosphere. Knowledge of these properties will affect both the camera system design and the photographic mission plan.

In the case of the moon a reasonably accurate photometric function, based on telescopic data, was available prior to the Ranger missions. This empirical function described the average* surface brightness as a function of the sun-surface-observer geometry. Since the shape of the mean lunar surface is a sphere so far as earth-based brightness measurements are concerned, this is equivalent to determining brightness of an average surface element as a function of the angles between the normal to the surface, the incident illumination vector, and the emitted illumination vector. Laboratory measurements have indicated that the apparent brightness is determined intrinsically by the small scale properties of the lunar surface material, such as the opacity, size, and packing density of individual particles or grains. Lacking an atmosphere, the photometric function for the moon is completely determined by its near surface properties.

Our present knowledge of the photometric properties of Mars is based on both telescopic data and the Mariner IV television experiment results. As Mars subtends about 1/3 minute of arc from earth during its best viewing periods (compared to 1/2 degree of arc for the moon) and is limited to phase angles (the sun-Mars-Earth angle) of 47° or less, it is not surprising that a photometric description comparable in detail to that of the moon was not available in advance of Mariner IV. One of the better compilations of "Mars photometric data" consists of a brightness map at a resolution of 10° (planet central angle) covering all longitudes and latitudes in the range ±60°[1]. The brightness for each 10° sector is an average of observed values taken as the position

---

*"Average" in a spatial sense, as the experimental determination of lunar surface brightness was limited spatially by the resolution achievable with earth-based instruments.

of the sector relative to the sun and earth changed due to both the diurnal rotation of Mars and the motion of the Earth and Mars about the sun. The resultant map is far from a description of the average surface brightness as a function of sun-surface-observer geometry.

The television experiment results returned by Mariner IV provide photometric data on Mars over a limited range of illumination and emittance angles at a resolution considerably better than earth-based observations. This is useful data for model fitting in any attempt to develop a self-consistent photometric description of Mars, although there are questions as to whether all of the Mariner IV photographic data should be accepted.

The objective of the present study is to provide a photometric description of Mars which can explain the Mariner IV data. The study has proceeded along two basic lines: (a) an analysis of Mariner IV data to develop criteria for photometric model building, including an analysis of the validity of the data (Section II); and (b) development of a model for the Mars surface and atmosphere which seems physically realizable and agrees in general with the above criteria based on the Mariner data as reported (Section III).

This report is considered preliminary in the sense that the scope is limited to consideration of the Mariner IV data. Further work will attempt to fit the present model to certain earth-based data, such as the geometrical albedo and the phase function (integral planet brightness as a function of phase angle). Additional checks on the validity of the model which can be made using Mariner '69 imagery are pointed out in Section IV.

II. Mariner IV Data

A. Empirical Basis for a Photometric Model of Mars

1. Feature Detection

One of the most important classes of data from the Mariner IV pictures is the variation from picture to picture of the number of surface features detected by trained observers. Assuming that the camera operated nominally and that the distribution of features on the surface is reasonably uniform, this data indicates the manner in which changing camera and lighting geometry affects the detection of topographic features. A photometric model of Mars should account for this change in feature detection.

Figure 1 indicates the number of craters and the number of central peaks counted in the retouched picture pairs made from the Mariner IV data[2,3]. These histograms confirm the generally held impression that the pictures near the center of the sequence revealed more surface detail. Figure 2 shows that the same trend occurs when the craters are grouped according to size (with the exception of an anomalously large number of craters with diameters D greater than 32 kilometers in frames 3 and 4). Marcus detected craters in the 4 to 5.6 kilometer size range for all pairs of frames from 3 and 4 through 13 and 14. This compares favorably with the theoretical camera resolution of 3 kilometers and indicates that the change in feature detection was not caused by a change in resolution.

When the number of craters detected per pair is plotted versus incident sun angle as in Figure 3, a peak occurs at about 40°. As the incidence angle increased from 40° to 60° the number of craters detected decreased by about a factor of two. Over this range the camera angle ε remained nearly constant (22 ± 2°) and the range from the camera to the surface varied only about ±3% from an average of 12,600 km. It appears that the lighting incidence angle strongly affects feature detectability within this range. It is possible that the reduced feature count is caused by an actual reduction of the number of surface features within the camera field of view. However, the reduced feature counts do not correlate well with any change in terrain type (e.g., light and dark areas) either on earth-based or the Mariner photographs. Moreover, the continued decrease in feature count as the angle of incidence increased toward the terminator strongly suggests that an interaction of the camera properties and Mars photometry reduces surface feature dectectability at high incidence angles.

2. Surface Brightness

The average brightness of the surface appearing in the Mariner IV pictures is a second class of data which must be accounted for by a Mars photometric model. Figure 4 shows the average brightness of the surface* as a function of incidence angle. The brightness is averaged over the area of surface included in a single picture; this is the data presented in Table III-6 of Reference 3. The "error bars" indicate the range of incidence angles in a single picture; these data are

---

*What is meant here is, of course, the apparent surface which includes the real surface modified by effects due to the atmosphere between the surface and the camera.

from Table D-4 of Reference 3. The unit of brightness is a millilamb, which is 10^{-3} times the brightness of a white Lambert surface normal to the sunlight at Mars.

The Mariner IV camera took pictures in overlapping pairs with alternate green and orange filters so that a pair consisted of a "green" and an "orange" picture. The color of the filter used in taking each picture is indicated on Figure 4. The camera was calibrated to account for different sensitivities with the different filters. The consistently greater brightness of the orange pictures reflects the fact that the brightness of Mars increases with wavelength. The camera spectral response was centered at $\sim$5300 Å with the green filter and at $\sim$6100 Å with the orange filter. According to Figure B-13 of Reference 3, the brightness of Mars is about 1.6 times as great at 6100 Å as at 5300 Å. If the brightness of the green pictures is multiplied by 1.6, they agree well with the brightness of the orange pictures as indicated in Figure 4.

Averaging the brightness data over the surface visible in one picture is sufficient to remove the brightness variations caused by topographic features, but more extensive brightness variations caused by albedo differences are still evident. Pictures 8 through 13 seem to depart from the curves established by the other pictures. According to Figure D-3 of Reference 3, these pictures contain parts of the Mare Sirenum. Other than this, the brightness appears to decrease monotonically with increasing incidence angles.

3. Sky Brightness

The third category of Mariner IV data involves the brightness of the illuminated atmosphere or sky. Unless refuted, the sky brightness data must be explained by the Mars photometric model. Figure 5 is a duplication of Figure III-15 in Reference 3 and shows the sky brightness above the limb of Mars. These data come from picture 1 in which the illuminated sky appears against the dark background of space. The sky 150 km above the limb appears about 60% as bright as the surface at the limb. Picture 1 was taken with an orange filter, hence these data reflect a camera spectral response centered at $\sim$6100 Å.

Figure 6 is a duplication of Figure III-16 in Reference 3. It shows brightness, presumably scattered from the atmosphere, as a function of the lowest directly illuminated altitude. Even with no direct sunlight illumination below 100 to 200 km, picture 22 indicates the presence of some atmosphere or other light scattering media at 200 km above the surface.

B. Validity of Mariner Photometric Data

Even a cursory examination of the calibrated but unenhanced Mariner IV pictures reveals two important characteristics: the contrast is extremely low and the sky in picture 1 is very bright. Both characteristics lead to the impression that there is substantial stray light in the pictures either from "haze" around the planet or "glare" in the camera, or perhaps a combination of these. The "haze" would be an important part of the photometric model of Mars while camera "glare" is just an effect of the measuring instrument.

Numerous arguments as to whether the stray light is due to planet haze or camera glare are given in Reference 3. Many of these arguments concern the likelihood of a particular occurrence and are not definitive. Therefore, the cause of the stray light is still in question. However, the following facts are known:

1. Some "veiling glare" existed in the camera optics, although it is not enough to account for the observed stray light.

2. It is possible to degrade the optics to produce effects similar to the stray light without greatly reducing the image brightness.

3. The stray light does not originate within the camera electronics since pictures of the dark sky made weeks after encounter are black. Magnification of the existing optical glare by electronic distortion has not been ruled out.

4. Some image retention from picture to picture occurs; it was estimated at about 10% from picture 1 to picture 2.

From this it is possible to say that at least some of the stray light originated within the camera as veiling glare. The following analysis is presented to indicate that, at least in picture 1, most of the stray light could have originated within the camera.

According to Reference 3, the Mariner IV encounter photographic sequence was initiated by a device called the Narrow Angle Mars Gate (NAMG). The NAMG[4] is a small telescope with an aperture of 1/2 inch and a rectangular field of view of 1 1/2° by 2 1/2°. Its optical axis is aligned with the camera optical axis. It was designed to start the photographic

sequence when the limb of Mars had moved a few tenths of a degree into its field of view. The light sensitivity specified to trigger the NAMG was 30 foot - lamberts (5.7 millilambs) over the entire field of view, or a point source which produced an equivalent amount of light.

The time at which the NAMG started the photographic sequence was obtained from JPL[6]. The times at which the first two photographs were taken are given in Reference 3, Table C-1. By extrapolation, shown in Figure 7, the relationship of the NAMG field of view to the camera field of view for pictures 1 and 2 can be found. The limb of Mars seen in picture 1 is shown. The limb is somewhat skewed because the aiming point was not exactly as planned, but otherwise the encounter was nominal. The NAMG started the photographic sequence when the limb encroached a few tenths of a degree as planned, and the first picture included the limb, as was desired.

The fact that the NAMG apparently performed nominally despite the unexpected brightness of the sky in Mariner picture 1 suggests that the sky brightness was due largely to camera glare rather than haze on Mars. If the sky and planet brightness indicated by picture 1 is integrated over the field of view of the NAMG at the time it triggered the photo sequence, the illumination of the detector is found to be about five times the value required to trigger the first picture. Figure 8 shows the brightness curve used to obtain this result. The solid part of the curve is the data from Reference 3 reproduced in Figure 5. The curve was extended below the limb on the basis of the average brightness of the planet in picture 1 as given in Reference 3 and by inspection of the brightness variation on the reproduction of picture 1. The sky brightness was abruptly terminated at 175 km above the limb - just beyond the edge of picture 1.

Mariner picture 1 was taken with an orange filter, hence the camera response was centered at $\sim$6100 Å. The spectral response of the Mariner Earth sensor, which used a Cd-S sensor like the NAMG, was centered at about 6000 Å. No correction for different spectral response between the camera and NAMG was made.

The five fold discrepancy between the brightness seen by the NAMG, indicated by picture 1, and the brightness required to activate the NAMG is the minimum consistent with the known uncertainties in the data. Terminating the sky brightness just beyond the edge of picture 1 reduces the brightness in the NAMG

field of view as much as possible. Using the earliest possible NAMG acquisition time also reduces the amount of light in the field of view. The 30 foot - lambert threshold for the NAMG is apparently the minimum sensitivity of the instrument; testing showed it had a tendency to become more sensitive with time by as much as a factor of three[4]. This would make the discrepancy even greater.

If we consider that the NAMG data is correct, the question arises as to how picture 1 might be corrected to bring it into agreement. If it is assumed that a uniform glare level exists in the picture, it is possible to compute a glare level which makes the photographic data and the NAMG data agree. This computed glare level, based on the conservative assumptions stated above, is 100 millilambs. If this brightness level were subtracted from picture 1, it would leave only a small amount of brightness in the sky at 150 km above the limb and would increase the contrast between the sky and the planet. The planet brightness would be approximately halved.

Since it has been determined experimentally that it is possible to degrade the camera optics to produce a large amount of veiling glare (which would appear as sky brightness) and not greatly change the apparent brightness of the planet, an alternate scheme for correcting picture 1 would be to disregard the sky brightness and leave the planet brightness unchanged. If the brightness curve in Figure 8 is assumed to be zero above the limb, the picture brightness and the NAMG data agree within about 15%. This very small discrepancy can be accounted for by the uncertainty in the camera photometric calibration.

If the NAMG data is accepted, it is possible to make the following conclusions about the sky and planet brightness data provided by picture 1. Most of the sky brightness appears to be due to camera glare and it is possible that the actual sky brightness is negligible. The actual planet brightness may be essentially as pictured or may be only about half as bright as pictured.

A series of discussions has been carried out with JPL over the past two months in an attempt to resolve the NAMG problem. The conclusion is that in view of the difficulty, or in some cases impossibility, of recovering critical data at this time, the discrepancy remains unresolved. The opinion of the Principal Investigator (R. B. Leighton, California Institute of Technology) is that the television data as reported is the best that can be made available prior to Mariner '69. It is the reported data which has formed the basis for the model work, with no corrections to bring the NAMG and camera brightness data into agreement.

III. Photometric Models Based on Mariner IV Data

A. Atmosphere

The brightness above the limb and the lack of contrast were unexpected results. These data can be explained by an atmosphere which is optically fairly thick. A fog on earth, for example, produces similar effects over much shorter distances. The known atmosphere of Mars, i.e., an atmosphere consisting principally of CO_2 and having a surface pressure of 5-10 mb and a scale height of 10 km, is completely inadequate to explain the reported phenomena.

In the subsequent sections, the term atmosphere should be taken to mean not the usual gaseous atmosphere, but some unspecified material like dust which will have the optical properties required to explain the Mariner IV data. This atmosphere will be described by four parameters: the scale height, a cutoff height, an extinction coefficient, and a scattering coefficient.

The density, d, of the atmosphere is taken to have the form

$$\begin{aligned} d &= d_o e^{-h/h_o} && \text{for } h \geq h_{co} \\ d &= 0 && \text{for } h < h_{co} \end{aligned} \qquad (1)$$

where d_o is the density extrapolated to the planetary surface, h is the altitude above the surface, h_o is the scale height, and h_{co} is the cutoff height. Figure 9 illustrates this density profile.

The exponential portion of the density profile has been chosen in analogy to the behavior of gaseous atmospheres, for which such profiles provide reasonable agreement. It was found necessary to include a low altitude cutoff in order to obtain agreement between the model and picture 1 from Mariner IV, specifically, to make the limb visible against the bright sky background. The rationale for this is discussed later in this section.

It is not possible to specify an exact criterion for the altitude profile of the brightness in the model. The observed brightness from Mariner IV extends to at least 150 km. The parameters of the model have been chosen so that the atmospheric brightness decreases rapidly above 200 km.

The extinction coefficient represents the fraction of a beam of light which is removed from the beam, per unit

length, by absorption and scattering. If F is the flux in a beam,

$$dF = F\sigma dx \tag{2}$$

where σ is the extinction coefficient and dx is an element of path length along the beam. The extinction coefficient is taken to be proportional to the density of the atmosphere and has the same analytical form as Equation (1) where σ_o is defined as the extinction coefficient extrapolated to the planetary surface. A scattering coefficient b and extrapolated surface valve b_o are similarly defined. The scattering coefficient determines the portion of the incident beam which is scattered (only) out the beam of light.

If a small volume element dV is illuminated by a beam of intensity S (lumens/unit area), the scattered light forms a point source of intensity dI

$$dI = \frac{b}{4\pi} SdV \tag{3}$$

where I is measured in candles if S is in lumens/unit area. The dimensions of b are $(\text{distance})^{-1}$. Scattering is assumed to be isotropic.

The extinction coefficient must be greater than or equal to the scattering coefficient because the extinction coefficient includes the process of scattering plus that of absorption. That is,

$$\sigma_o \geq b_o \tag{4}$$

B. Surface

For the purposes of the model calculations the photometric properties of the Martian surface are taken to be those of a Lambert surface with a normal albedo ρ_o. All of the calculations are carried out with the same albedo, although it is clear that for some of the pictures the scene photographed was a dark area of Mars, and a lower albedo would be appropriate.

There is little earth-based data upon which to base a choice of photometric properties of Mars. One example of

available data is the phase function (5), which is in agreement with a model consisting of a lunar-type reflective surface plus a thin atmosphere. Such a deduction about the surface properties is not applicable to the presently postulated model in which atmospheric effects significantly modify the photometric appearance of the surface.

C. Values of the Parameters

The set of parameters given in Table I has been chosen to give a good fit to the data obtained from Mariner IV. The relationship between the parameters and the data and the logic which led to the particular choice of parameters will be discussed in some detail in parts of this section.

TABLE I

Scale height	h_o	75 km
Cutoff height	h_{co}	50 km
Extinction coefficient	σ_o	.01/km
Scattering coefficient	b_o	.006/km
Surface normal albedo	ρ_o	0.5

D. Slope Sensitivity Calculations

Slope sensitivity relates changes in the signal produced by the camera to changes in the slope of the surface. It depends on the photometric properties of the surface, the transmission properties of the atmosphere and the camera system. Geometric and atmospheric conditions which produce a high slope sensitivity lead to pictures with readily discernible surface detail compared to pictures in which the slope sensitivity is low.

Figure 3 illustrates the detection of craters in the Mariner IV pictures. This figure may be interpreted as indicating that in pictures taken at incidence angles of about 40 degrees, the slope sensitivity is higher than at other incidence angles. The photometric model postulated here gives qualitative agreement with the results indicated in Figure 3. Lack of knowledge of the surface topography, along with other reasons, prevents any quantitative comparison.

The slope sensitivity G (i,ε) is a function proportional to the change in camera signal divided by the slope difference producing the change. The angle i is the angle between the local vertical and the incident radiation, and ε is the angle between the local vertical and the direction to the observer. Because of the particular properties of the Lambert surface, which is used in this model, the slope sensitivity does not depend on the phase angle.

Although slope sensitivity depends on the response of the camera system, there is inadequate information presently available to account for the effect reliably. For this study the response of the camera is assumed to be constant and linear. Under these assumptions, the camera parameters do not enter the slope sensitivity calculation.

The slope sensitivity is most easily calculated by considering the case where there is no atmosphere, and then by modifying the result to account for the effect of the atmosphere. The geometry is shown in Figure 10. The slope sensitivity with no atmosphere, s(i), is given by

$$s(i) = \left[\left|\frac{\partial B}{\partial k}\right|_{k=0}\right] \text{ average over } \omega \qquad (5)$$

where B is the surface brightness and k the angle between the local vertical and the normal to the sloping surface. The derivative is evaluated at k=0 since that represents a flat surface at the local area. The derivative is averaged over the azimuthal angle ω under the assumption that slopes are equally probable in all directions. The absolute value of the derivative is taken before averaging because, for the purpose of slope detection, brightness decreases are as useful as brightness increases. The function s(i), plotted in Figure 11, can be defined as the average (over the azimuthal angle) of the absolute value of the rate of change of the surface brightness as the surface is tilted away from local vertical. Thus s(i) is a reasonable measure of the brightness change produced by the terrain in a region. Where there are limits on the detection of brightness differences, as exist in all real systems, slopes which produce large brightness changes are more easily detected than those in other areas. Therefore the slope sensitivity is a reasonable measure of the expected quality of the pictures.

The presence of the atmosphere alters the slope sensitivity through two principal effects. First, it decreases the intensity of the incident sunlight reaching the surface, and second, it attenuates the light reaching the camera from

the surface. Both of these effects reduce the brightness of the entire local area by a constant factor, and hence also reduce the brightness difference between surfaces having different slopes.

The change in the apparent brightness B of the surface seen through an atmosphere is given by

$$dB = B\sigma dx = B\sigma_o e^{-h/h_o} dx \tag{6}$$

and,

$$B = B_o e^{-\sigma_o \bar{R}_c} \tag{7}$$

where B_o is the brightness if no atmosphere were present and

$$\bar{R} = \int_{h_{co}}^{\infty} e^{-h/h_o} \frac{dx}{dh} \, dh \tag{8}$$

$\bar{R}$ is a function of the angle between the line of sight and the local vertical. The function is plotted in Figure 12. $\bar{R}_c$ denotes the value of $\bar{R}$ along the line of sight to the camera.

Similarly, the intensity of the incident sunlight may be shown to be

$$S = S_o e^{-\sigma_o \bar{R}_s} \tag{9}$$

where $\bar{R}_s$ is the value of $\bar{R}$ along the line of sight to the sun, S_o is the unattenuated intensity of the incident solar radiation, and S is the value at the surface.

Both the attenuation of the incident sunlight and the attenuation of the scattered sunlight reduce the slope sensitivity $G(i,\varepsilon)$, which becomes

$$G(i,\varepsilon) = s(i)e^{-\sigma_o \bar{R}_c(\varepsilon)} e^{-\sigma_o \bar{R}_s(i)} \qquad (10)$$

The functions G and s are plotted in Figure 11 as a function of the incidence angle, although the function G depends on both the incidence and emittance angles. The incidence angle was chosen as a convenient parameter to separate the Mariner IV pictures, and at each point the emittance angle ε was chosen in agreement with the trajectory data. A similar convention will be employed in the subsequent figures.

The additional illumination of the surface produced by sunlight scattered from the atmosphere does not contribute appreciably to the ability to detect slopes and has not been included in the slope detection calculations. The scattered sunlight is almost uniform over the sky hemisphere, as seen from a point on the surface of the planet, and surfaces which are vertical receive the same illumination from scattered sunlight independent of the direction in which they are tilted.

The slope sensitivity does not depend on the parameter b_o nor on the albedo ρ_o. In the latter case, this is because ρ_o is taken to be the same constant in all pictures, and therefore, as a multiplicative factor, it does not affect the relative picture quality. The parameter b_o affects the brightness of the atmosphere, but does not degrade the slope sensitivity. This is because the atmospheric brightness represents a constant background and does not contribute to the differential brightness change $s = \delta B/\delta k$. Degradation of slope sensitivity arises only from the extinction of light by the atmosphere.

The function $G(i,\varepsilon)$ (Figure 11) has the general shape required by the Mariner IV pictures; that is, it has a maximum in the center and falls off at either end. This is to be compared with the crater count curves in Figure 3, which also peak in the middle of the photo sequence. It is not possible to obtain quantitative data from Mariner IV to compare with this curve, since the actual topography is unknown. Only the shape of the curve is important.

To obtain the desired shape, it is necessary to choose a moderately thick atmosphere, i.e., the product of σ_o and $\bar{R}$ should be about unity. Thinner atmospheres than we have chosen would not provide as much roll-off for high incidence angles. This is illustrated by Figure 11 where s(i), which does not include atmospheric affects, increases mono-

tonically with increasing illumination angle, i.e., as the Mariner picture sequence approaches the terminator. On the other hand, too thick an atmosphere would entail such low contrast, relative to that expected with no atmosphere, that no detail at all would be expected in the Mariner IV pictures.

E. Brightness Calculations

The brightness calculations consider the effects of atmosphere seen above the limb in Mariner picture 1 and the appearance of the surface in pictures 1 through 19. A major problem in the interpretation of the Mariner IV pictures was that the brightness visible above the limb in picture 1 extended essentially undiminished from the limb to an altitude of at least 150 km. Since the rate of decrease was low, reasonable extrapolation of the curve would give rise to appreciable brightness at large distances, say 500 km, above the limb. Such an atmosphere should be detectable from earth. As there is no evidence for such an atmosphere, the model parameters h_o, σ_o, and b_o were adjusted to produce a rapid decrease in sky brightness beginning just above the region contained in Mariner picture 1 (i.e., about 150 km altitude). This decrease in model atmosphere brightness is illustrated in Figure 13.

A physical explanation for this atmospheric brightness profile is that near the limb, the viewer is unable to see all the way through the atmosphere. Looking farther above the limb, the atmosphere becomes thinner and the viewer sees farther into it, but still not all the way through. Because of this the brightness changes very little as a function of altitude above the limb for altitudes less than 150 km. However, once the density decreases so that the viewer can see completely through the atmosphere ($\sigma_o \bar{R} \sim 1$), then the apparent brightness of the atmosphere will decrease rapidly at a rate commensurate with the scale height, h_o.

The calculations of the atmospheric brightness took into account single but not multiple scattering. That is, each volume element was assumed to be illuminated with sunlight attenuated in passing through the atmosphere. The illumination of the volume element produced by scattered sunlight was ignored. The attenuation of the light between the volume element and the camera was taken into account.

Figure 13 illustrates results of the calculations. The selection of σ_o and h_o was made to explain the slope sensitivity data (i.e., the pictures in the middle of the

sequence appear clearer) and the atmospheric profile (i.e., the shape of the curve for brightness vs. altitude above the limb). The parameter b_o adjusts the amplitude of the atmospheric brightness. Initially results were computed assuming that the atmosphere extended to the Mars surface. The data indicated that the thickness of the atmosphere looking tangent to the limb was so great that the limb could not be seen. The discontinuity in brightness at the limb is an essential feature of the model, since the limb is readily apparent even in the unenhanced Mariner pictures. This requirement led directly to the selection of a low altitude cutoff, h_{co}, below which the atmosphere is transparent. This produced the desired shape for the brightness profile below the horizon in Figure 13, and the value of ρ_o (albedo) was selected to provide a limb brightness discontinuity and general surface brightness comparable to Figure 5.

The necessity of introducing a cutoff altitude h_{co} was forced by the requirement to expose the limb of the planet. The resulting model atmosphere is one in which the light scattering elements are concentrated between about 50 km and 200 km above the surface (i.e., within a shell which is 2 scale heights thick). There may be some physical significance to this model in the following sense. Meteoroids entering the earth's atmosphere break up at altitudes around 100 km, providing a source of light scattering material. Noctilucent clouds have been observed at about the same region in the earth's atmosphere, demonstrating the existence of light scattering sources concentrated at high altitudes. It is quite possible that such mechanisms could be effective at Mars, and if so, comparable altitudes might be expected. Figure 14 compares the density of the earth's atmosphere with several possible models of the gaseous atmosphere proposed for Mars. The Mars models bracket the earth's density in the region around 100 km.

Figure 15 illustrates the illumination level at the Martian surface as a function of the incidence angle. As expected the atmosphere reduces the illumination due to direct sunlight, while the scattered light, or skylight, provides some illumination of the surface beyond the point which would have been the terminator in the case of no atmosphere (i.e., where the incidence angle equals 90°).

Model calculations for the surface brightness at the center of the Mariner IV pictures are shown in Figure 16, together with the contribution to the apparent brightness due to the atmosphere. These points have been calculated for a constant albedo ρ_o, so that the dip in the brightness curve in

the Mariner IV data (see Figure 4) caused by the dark surface areas is not included. The brightness difference between the calculated curve and the atmospheric contribution is proportional to the surface albedo.

The albedo was chosen to give reasonable agreement with Mariner IV brightness data. A single value produces quantitative agreement at the limb, as mentioned previously, (specifically, the magnitude of the discontinuity) and at the center of each of the Mariner IV pictures, to an accuracy of about 10%. However, the surface albedo is significantly higher than that of the moon, and it indicates an exceptionally efficient reflecting surface.

As Section II has raised the possibility of a significant amount of glare in Mariner picture 1, model computations were made for a case where the atmospheric scattering coefficient b_o was reduced by a factor of 10, while retaining the other parameters constant. The resulting brightness profile which would be deduced for Mariner picture 1 is shown in Figure 17. As expected, the brightness of the atmosphere decreased by an order of magnitude. Figure 18 illustrates the calculated brightness vs. incidence angle (or picture number) at the centers of the Mariner pictures for the same case. The critical features of the Mariner IV data are maintained in this model, including the brightness discontinuity at the limb and the fall off in picture brightness with increasing incidence angle. The brightness of the atmosphere 50 km above the limb was about 70% of the brightness at the center of picture 1 in Figure 16. This is reduced to about 15% in Figure 18, i.e., the haze above the limb appears less bright compared to the surface. The slope sensitivity calculation does not depend on b_o and therefore remains the same for this choice of parameters.

There is extensive freedom within the model to adjust parameter values and functional forms to make the fit to the Mariner IV data even more precise. The choice of a Lambert surface and an exponential density profile for the atmosphere are arbitrary, and there is considerable freedom in the choice of parameters describing the atmosphere.

The purpose of the model is to demonstrate that all of the relevant photometric data obtained from Mariner IV can by explained by a single photometric model, which includes a haze atmosphere. This model is sufficiently accurate that it appears justified to use the model to predict the photometric behavior of Mars in geometric configurations not photographed by Mariner IV.

This model is wholly dependent on Mariner IV data, and any adjustment of that data would be reflected in changes in the parameters of the model.

IV. Applications for Future Missions

A. Mariner '69 Flyby

Both far- and near-encounter limb photography on the 1969 Mariner Mars flyby mission should provide an important check on the validity of the Mariner IV data, and hence on the foundations for the haze model. Full planet far-encounter photography at relatively small phase angles ($\sim 30°$) will expose essentially half the circumference of the planet disk to a search for atmospheric haze. At a resolution of about 30 km/line pair this data should be adequate to determine whether any haze phenomenon of the magnitude apparent in the first Mariner IV picture exists.

Higher resolution limb photography could be obtained during the near-encounter photographic sequence. If the haze effect is confirmed, the sequence of full planet photography will provide evidence of its spatial and temporal variations.

B. Mariner '71 Orbiter

One of the objectives of the '71 imagery experiment is to search for temporal changes in the surface properties of Mars. In particular, the wave of seasonal darkening will be investigated, largely by searching for albedo changes in photographs of the same surface areas taken at different times. If the '69 data confirms that the haze model described here is substantially correct, there are important consequences bearing on the success of the '71 imagery experiment.

In particular, the model predicts an atmospheric contribution of about 25% to the scene brightness over an average mare 50° from the terminator, increasing to a contribution greater than that from the surface 10° from the terminator. This 10°-50° interval is approximately the range at which the swaths of periapsis photography will be acquired on the 1971 orbiter mission. Furthermore, over this range of angles, a 20% change in haze brightness would appear as at least a 5% change in apparent surface albedo. While temporal and spatial variations in the haze contribution are completely unknown at this time, this magnitude of change may well be induced merely by the varying sun/camera geometry which is required to repeatedly photograph the same surface areas throughout the orbital mission. It would seem that a 5% surface albedo change would be important to an investigation of the wave of darkening, considering that a 50% increase in albedo would make a mare as bright as a desert.

The haze can therefore make a significant contribution to the overall scene brightness (and brightness changes). One obvious use for the haze model, then, would be to subtract the haze effect from the pictures to expose the true surface brightness. Three types of pictures have been identified as being particularly appropriate to this extension of the model work for the '71 mission. The first is photography of the limb above the area of surface photographs taken on each orbit. This will expose the haze against the dark sky background. Second is photography of the terminator region just beyond the area of surface photographs to expose the illuminated haze against the dark planet surface. And third is a series of full planet photographs on approach in which the changing brightness contrast of pairs of bright and dark areas can be measured as the rotating planet varies the incidence and emittance angles. Assuming the same photometric function for the two surface areas, any observed changes in contrast should be due to atmospheric effects. Use of these data in formulating the haze model would not require knowledge of the surface photometry, as was the case with the Mariner IV data. In this case, once the surface pictures were corrected for the haze effect, an empirical model for surface photometry could be developed.

V. Summary

Examination of the Mariner IV television pictures and data derived from these pictures by JPL has led to the development of three criteria which can be used to test any proposed photometric model of Mars.

1. Histograms have been developed to reveal the number of craters and number of central peaks in most pictures of the Mariner sequence. These data confirm the observation that the pictures in the middle of the sequence reveal more surface detail than either those at the beginning or at the end. Feature detectability has been plotted as a function of picture number, or angle of solar illumination, as the picture sequence progressed towards the terminator.

2. Average surface brightness in the Mariner pictures has been tabulated by JPL. This data can also be plotted as a function of solar illumination angle, indicating a general trend of decreasing picture brightness as the sun approaches the horizon, i.e., as the picture sequence approaches the terminator.

3. Perhaps the most startling feature of the Mariner photos is the brightness of the sky in the first picture. The sky at 150 km above the limb, which is the highest altitude visible in the picture, is approximately 60% as bright as the limb. JPL has determined the absolute scene brightness as a function of altitude above and below the limb, and any photometric model for Mars should account for this feature.

In view of the surprising amount of sky brightness in the first Mariner picture, a separate study was conducted to test the validity of this data. It was concluded that if this brightness was a real property of Mars, then the amount of light seen by the Narrow Angle Mars Gate sensor was about 5 times the nominal threshold thought to be required. (The NAMG is an optical sensor separate from the vidicon system which responds to integral scene brightness). The amount of sky brightness reported would be sufficient to cause the first picture to be taken considerably earlier, thereby photographing a much larger portion of the atmosphere above the limb.

Several explanations of this discrepancy are possible. One is that the apparent sky brightness is glare in the camera system. This possibility was investigated by JPL with the conclusion that, in the laboratory, they could not find a reasonable mechanism for producing the observed brightness either with the nominal camera system or with one of degraded performance. Other sources of error are the time at which the NAMG achieved its threshold level of integral scene brightness, or the changing sensitivity of the photo-detector surface of the NAMG.

These questions have been pursued with JPL. It was concluded that the NAMG problem would remain unresolved due to lack of necessary data, and the best course of action for the model work would be to assume that the Mariner IV television data is correct as reported.

Four parameters were introduced to describe the properties of the atmosphere, where, by definition, atmosphere refers to the light scattering elements which are necessarily distinct from the gaseous atmosphere. Values chosen for the scale height and extinction coefficient effectively produced the observed decrease in sky brightness above 150 km and the enhanced slope sensitivity, which is related to the criterion of feature detectability, near the middle of the picture sequence. A value selected for the atmospheric scattering coefficient produced the correct magnitude of sky brightness above the limb. Finally it was necessary to introduce a cutoff altitude

(50 km) below which the density of light scattering elements was zero in order to make the limb of the planet visible. A single surface albedo of 0.5 produced the desired brightness discontinuity at the limb and the desired amplitude of the decreasing picture brightness as the photographs approached the terminator. The shape of this latter function is primarily determined by the assumed surface photometric function, although atmospheric effects are increasing in importance towards the terminator.

Although earth-based measurements of the Mars phase function indicate that a lunar photometric model for the surface might be appropriate in the case of a thin atmosphere, the true surface light scattering properties are concealed by the thick atmosphere which was found necessary to describe the Mariner data. With no real evidence to the contrary, a Lambert surface has been used to simplify the model computations.

The resulting model has a plausible physical explanation and fits the Mariner IV data criteria. One bothersome aspect is the high surface normal albedo. An obvious step in continuing this work is to determine quantities such as the phase function and geometric albedo for the model and compare them with earth-based observations.

VI. Conclusions

An empirical model for the photometric properties of Mars has been developed which can explain all the relevant features of the Mariner IV television data. A principal feature of this model is a haze component in the atmosphere. This haze has the effect of degrading the surface contrast and making the atmosphere visible above the limb and beyond the terminator. The magnitude of this haze effect was not predicted from earth-based observations.

The utility of a model such as this is two-fold. First, it may be used as a basis for further studies of the nature and possible origin of the haze. More importantly, however, it provides a technique for computing the haze effect on picture brightness. This would be necessary for any experiment which depends on a knowledge of surface albedo or albedo variations, since haze properties may vary in space and time.

Mariner '69 far-and near-encounter photography should provide a definitive check on the validity of the haze model for the Mars atmosphere.

Paul L Chandeysson

P. L. Chandeysson

E. N. Shipley

W. B. Thompson

W. B. Thompson

PLC
1014-ENS-mao
WBT

REFERENCES

1. "A Low Resolution Photometric Map of Mars", G. de Vaucouleurs, Icarus 7, 1967.

2. "Number Density of Martian Craters", A. Marcus, Bellcomm Technical Report # TR-68-710-1, January 29, 1968.

3. Mariner IV Pictures of Mars, R. Leighton et al., JPL Technical Report #32-884, December 15, 1967.

4. Mariner Mars 1964 Project Report: Mission and Spacecraft Development, Volume 1, JPL Technical Report #32-740, March 1, 1965

5. Planets and Satellites, Edited by G. Kuiper and B. Middlehurst, University of Chicago Press, 1961, p. 326.

6. A. Herriman, Jet Propulsion Laboratory, Personal Communication.

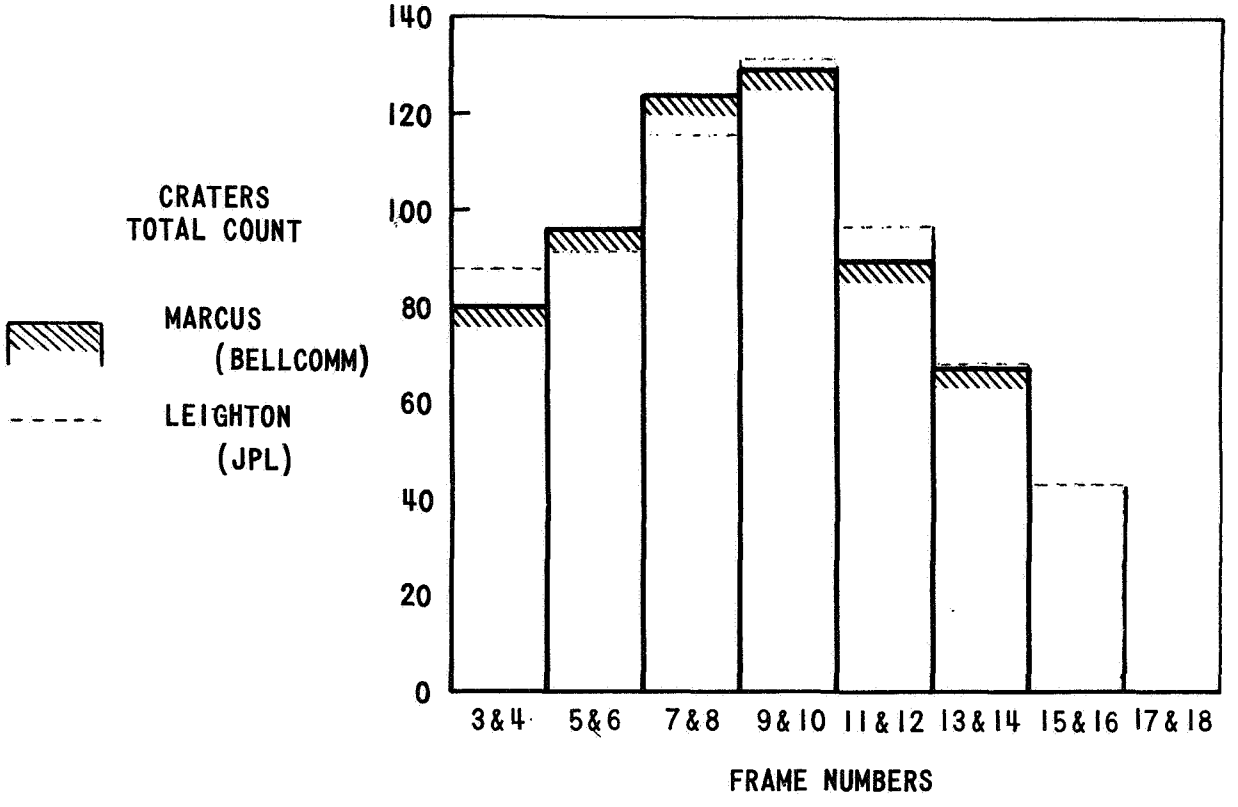

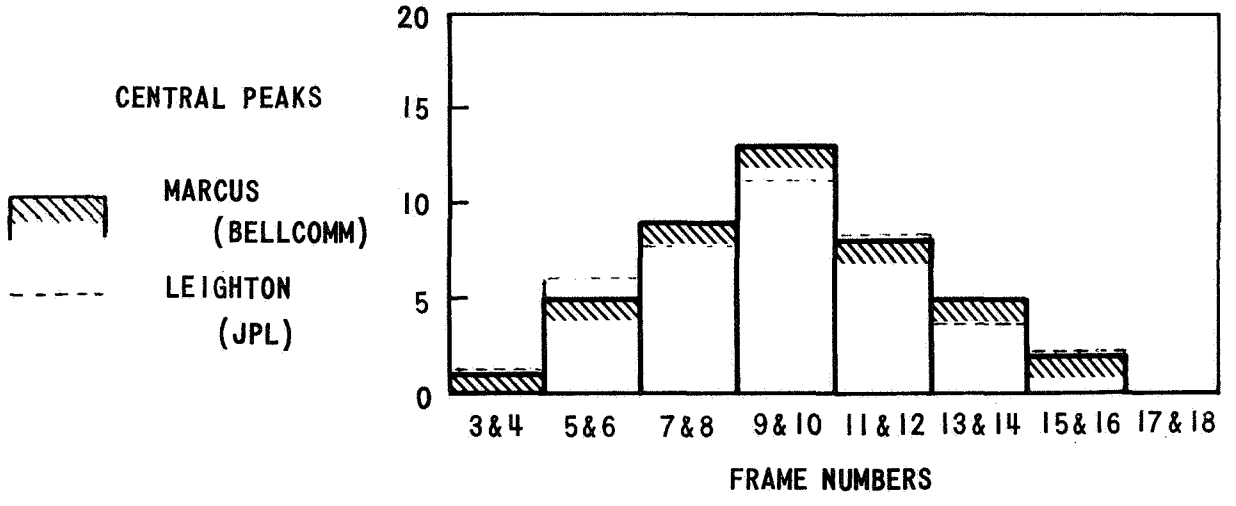

FIGURE 1 - FEATURES COUNTED IN MARINER IV PICTURES

MARCUS-BELLCOMM TR-68-710-1
LEIGHTON-JPL TR-32-884

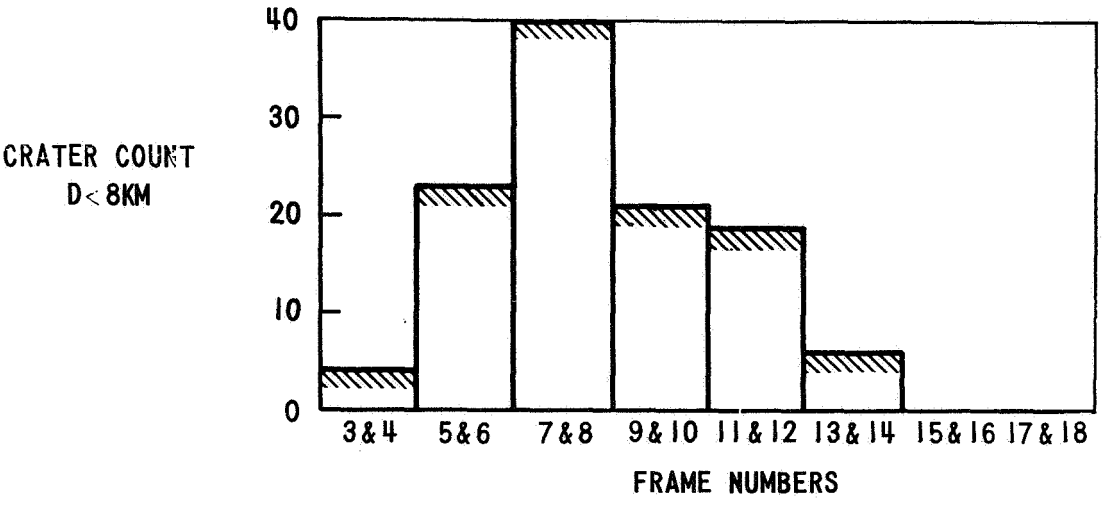

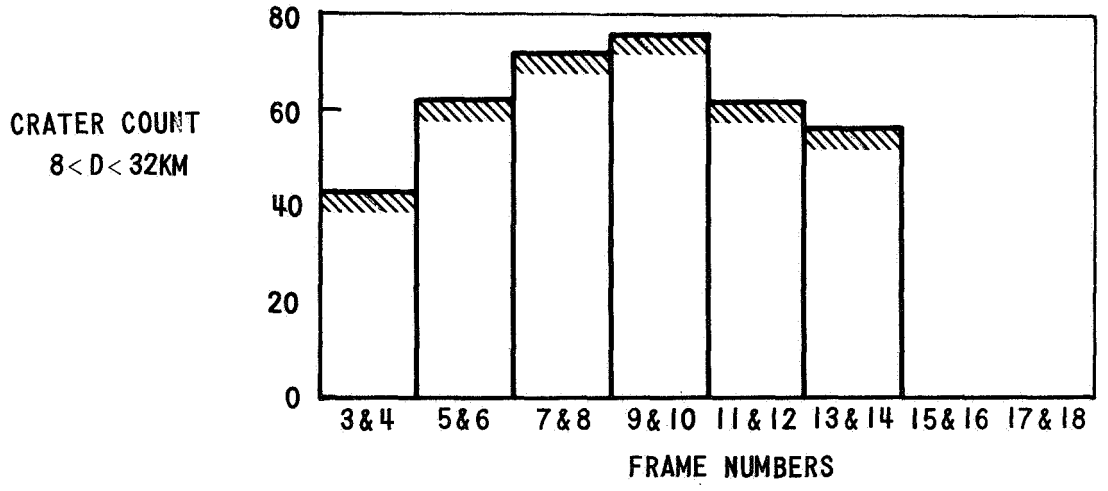

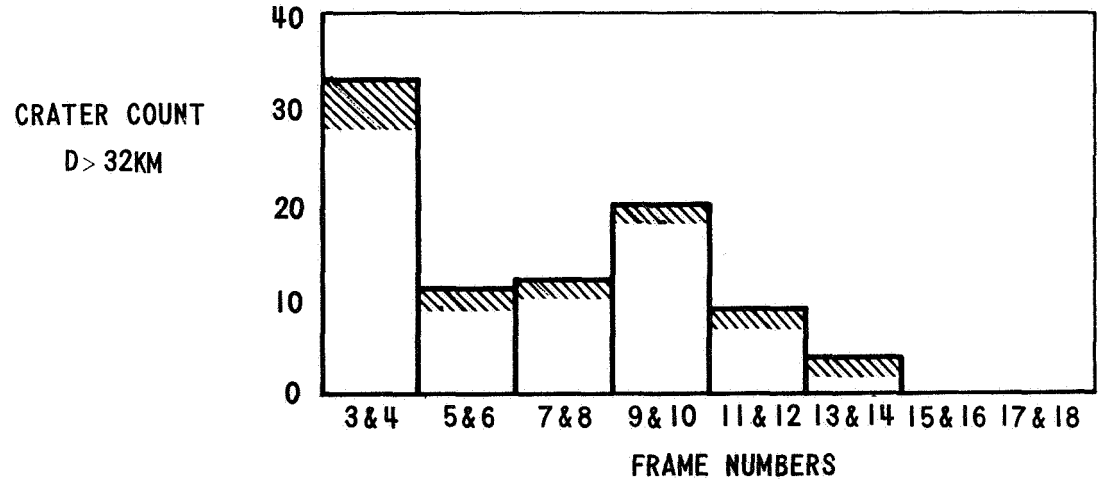

FIGURE 2 - CRATERS COUNTED IN MARINER IV PICTURES

DATA FROM MARCUS-BELLCOMM TR-68-710-1

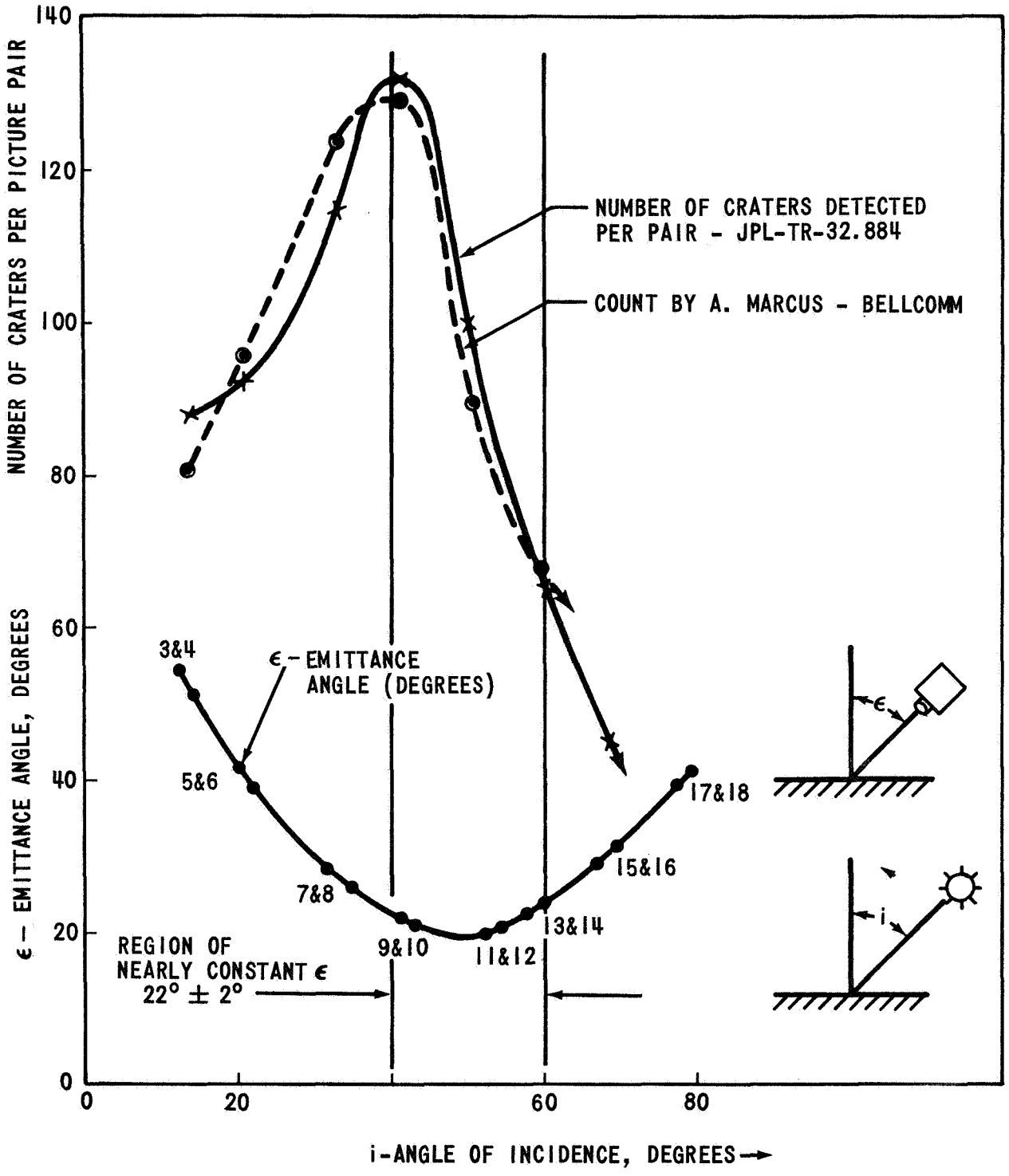

FIGURE 3 - CRATER DETECTION IN MARINER IV PICTURES

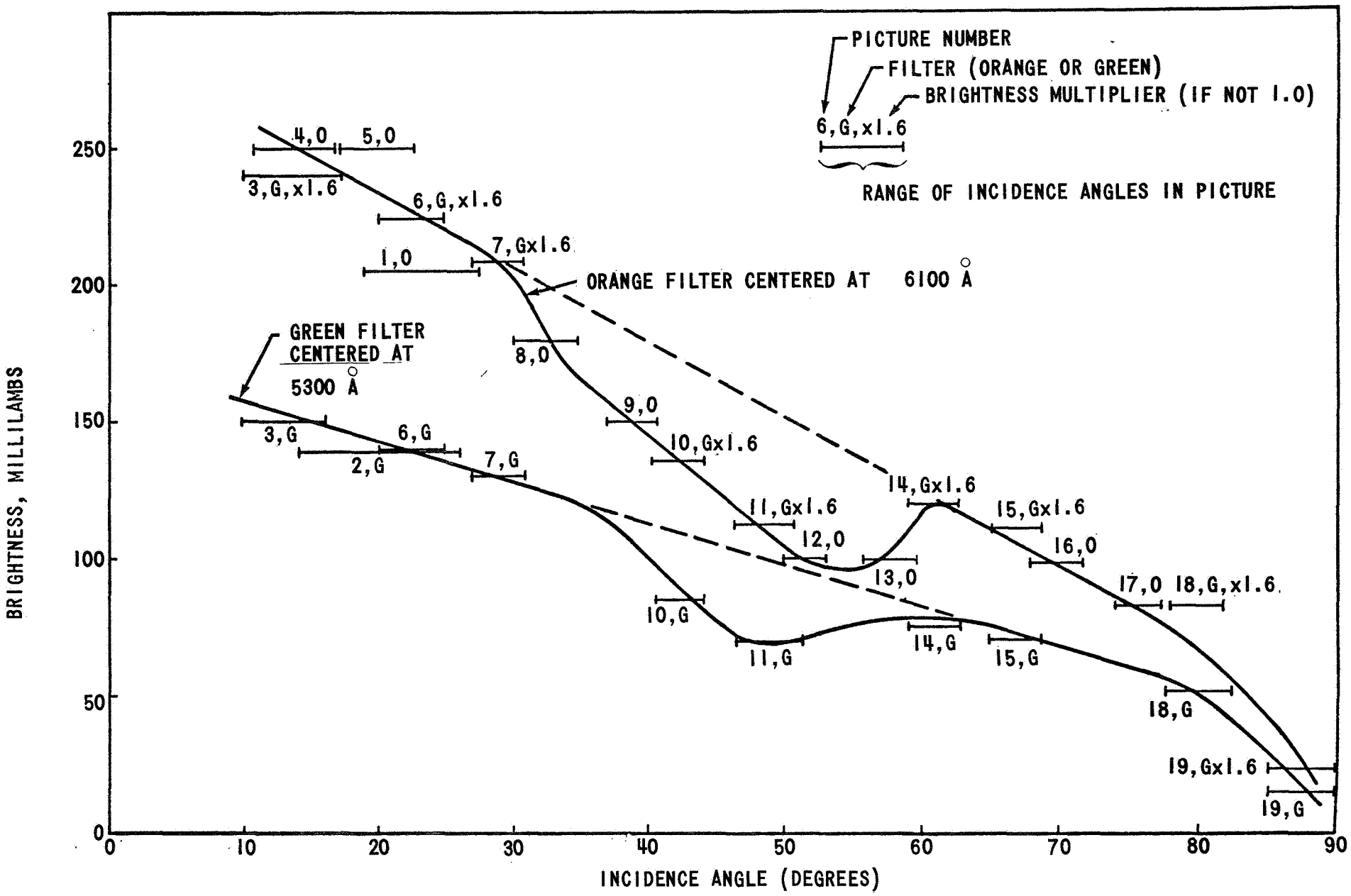

FIGURE 4 - AVERAGE SURFACE BRIGHTNESS vs. INCIDENCE ANGLE

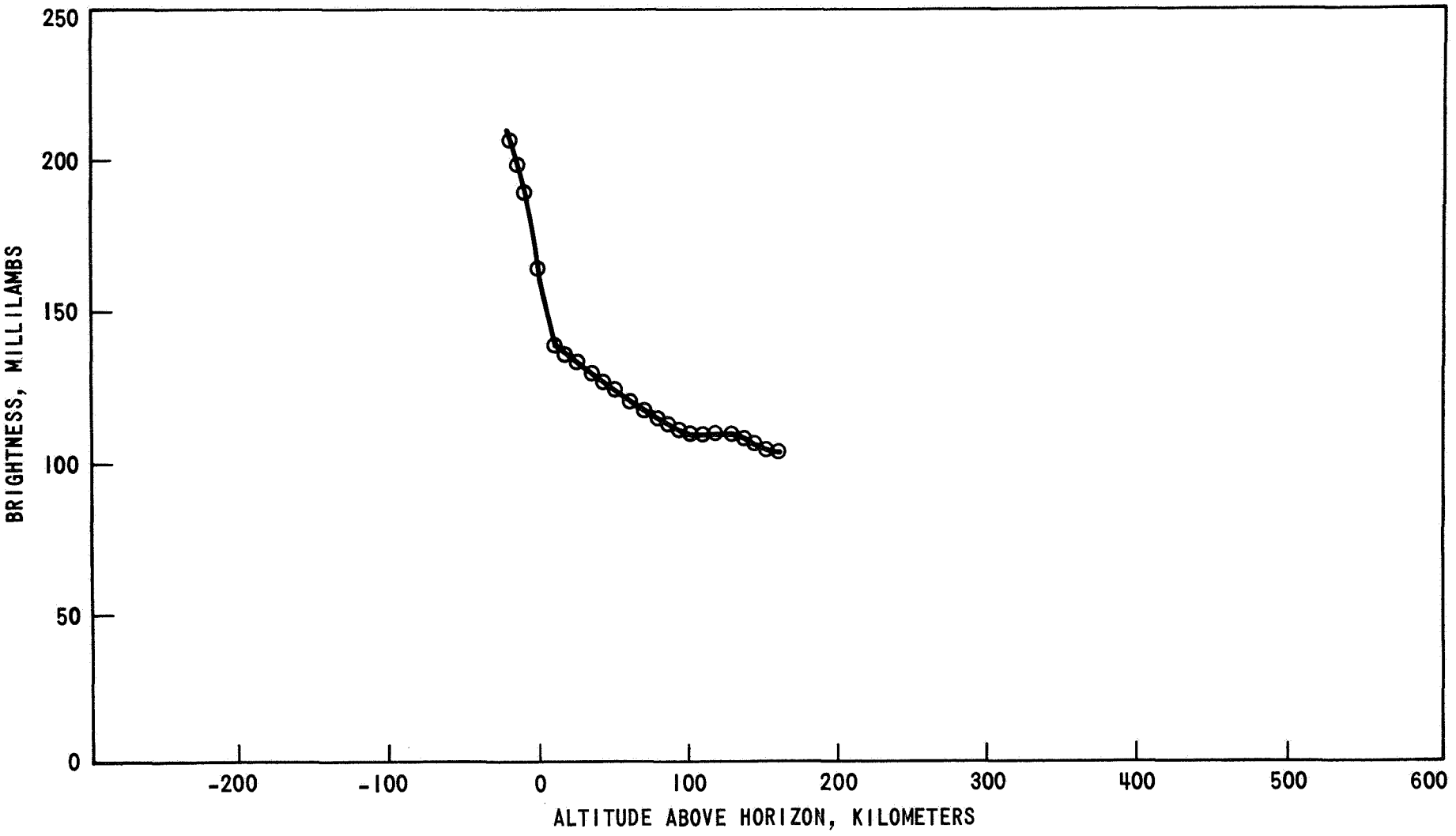

FIGURE 5 - MEASURED BRIGHTNESS PROFILE FROM MARINER IV PICTURE #1

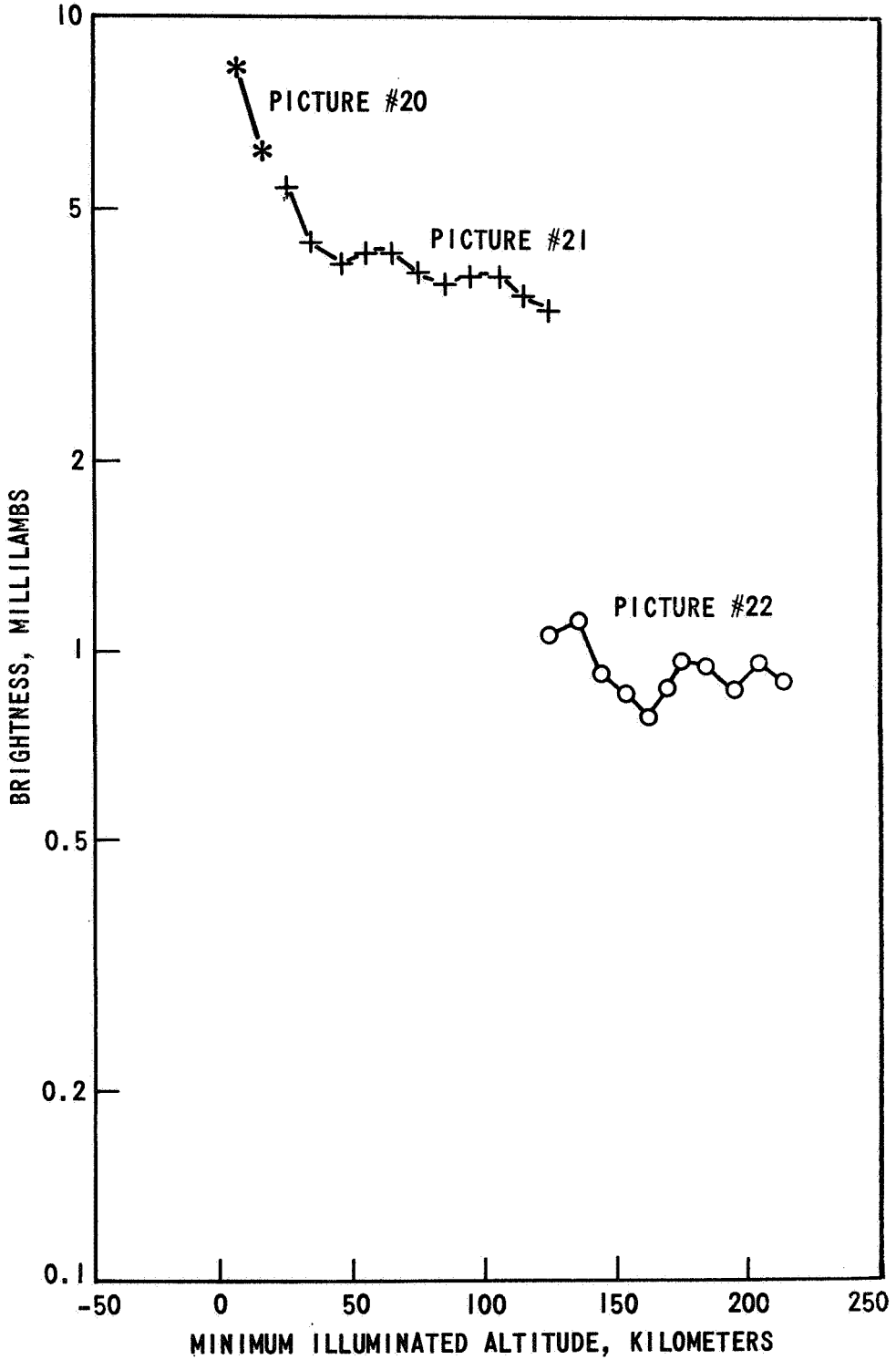

FIGURE 6 - MEASURED BRIGHTNESS VS. MINIMUM ILLUMINATED ALTITUDE IN THE ATMOSPHERE

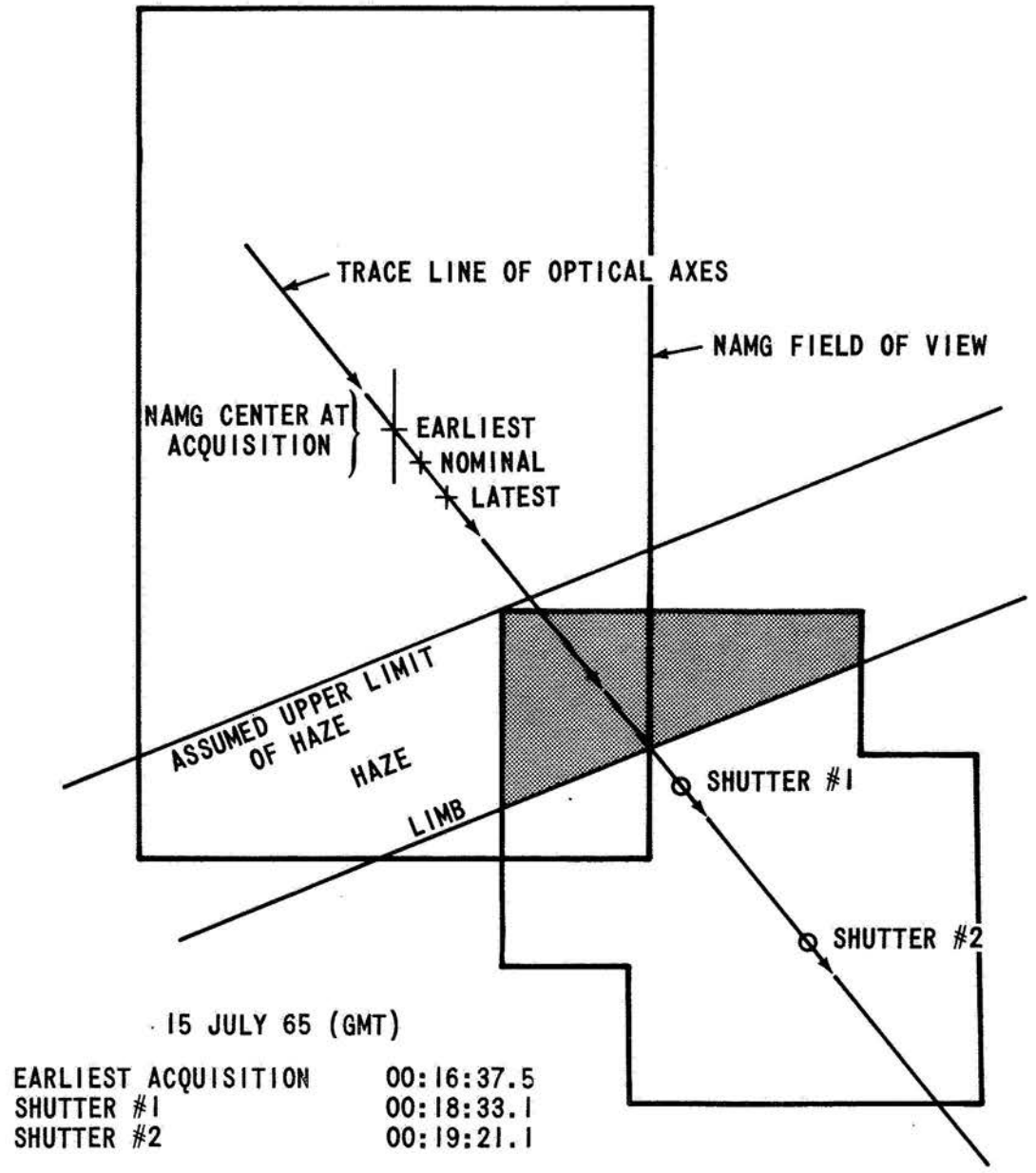

FIGURE 7 - LIMB POSITION IN NAMG FIELD OF VIEW AT ACQUISITION

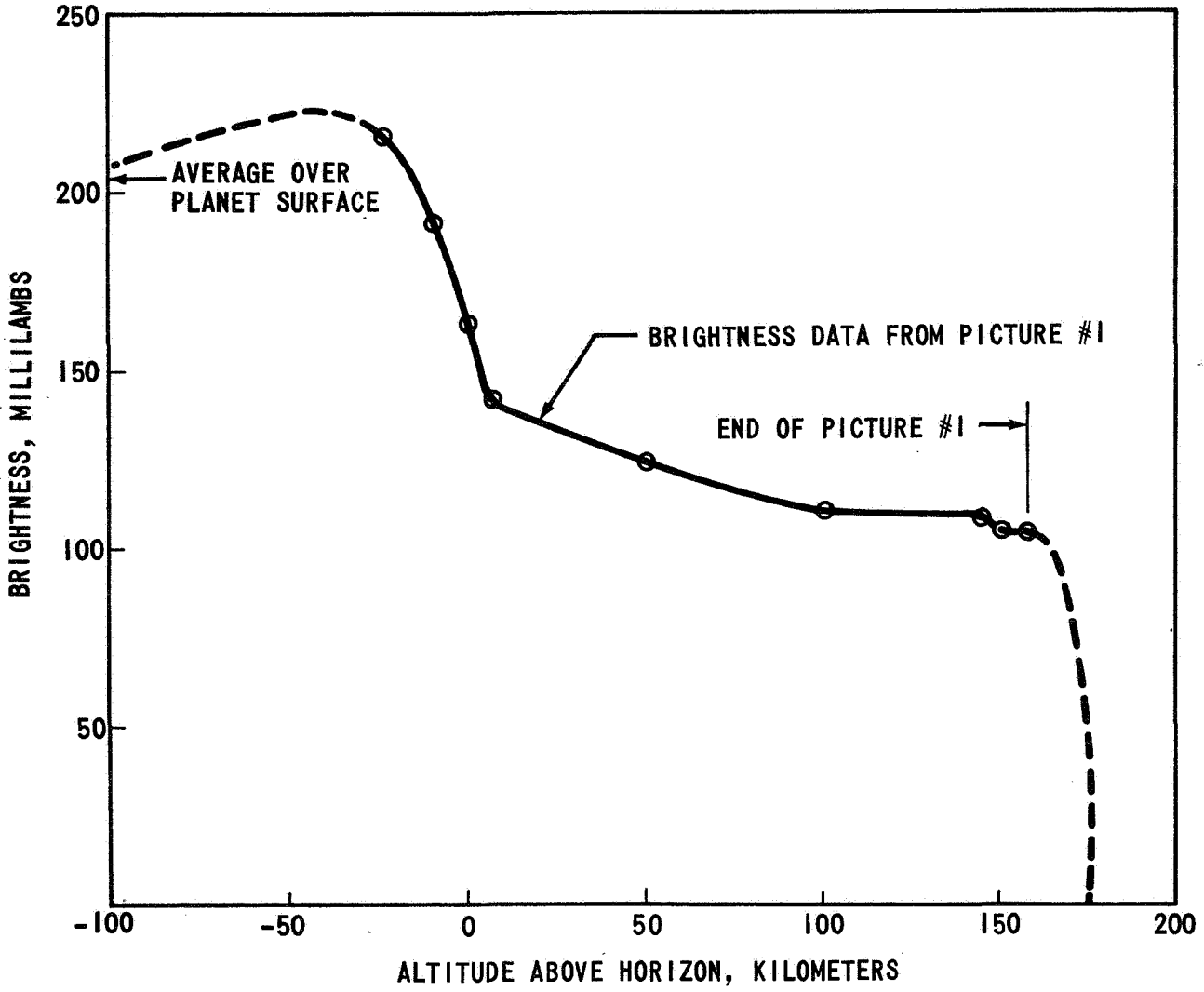

FIGURE 8 - BRIGHTNESS PROFILE ACROSS LIMB

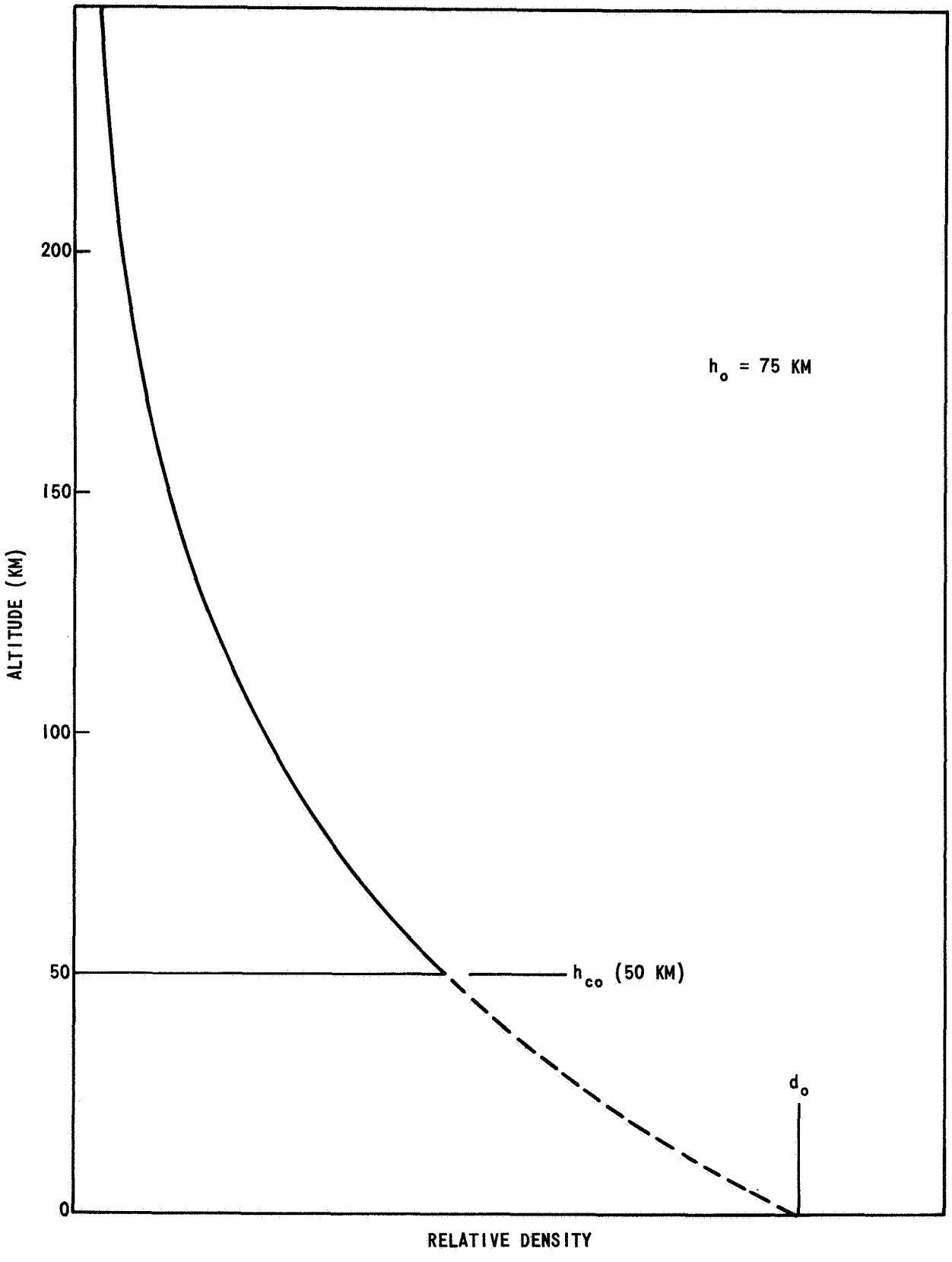

FIGURE 9 - DENSITY PROFILE OF SCATTERS SHOWING THE EXTRAPOLATED DENSITY d_o AND THE CUTOFF ALTITUDE h_{co}. THE EXTINCTION COEFFICIENT σ AND THE SCATTERING COEFFICIENT b ARE PROPORTIONAL TO THE DENSITY

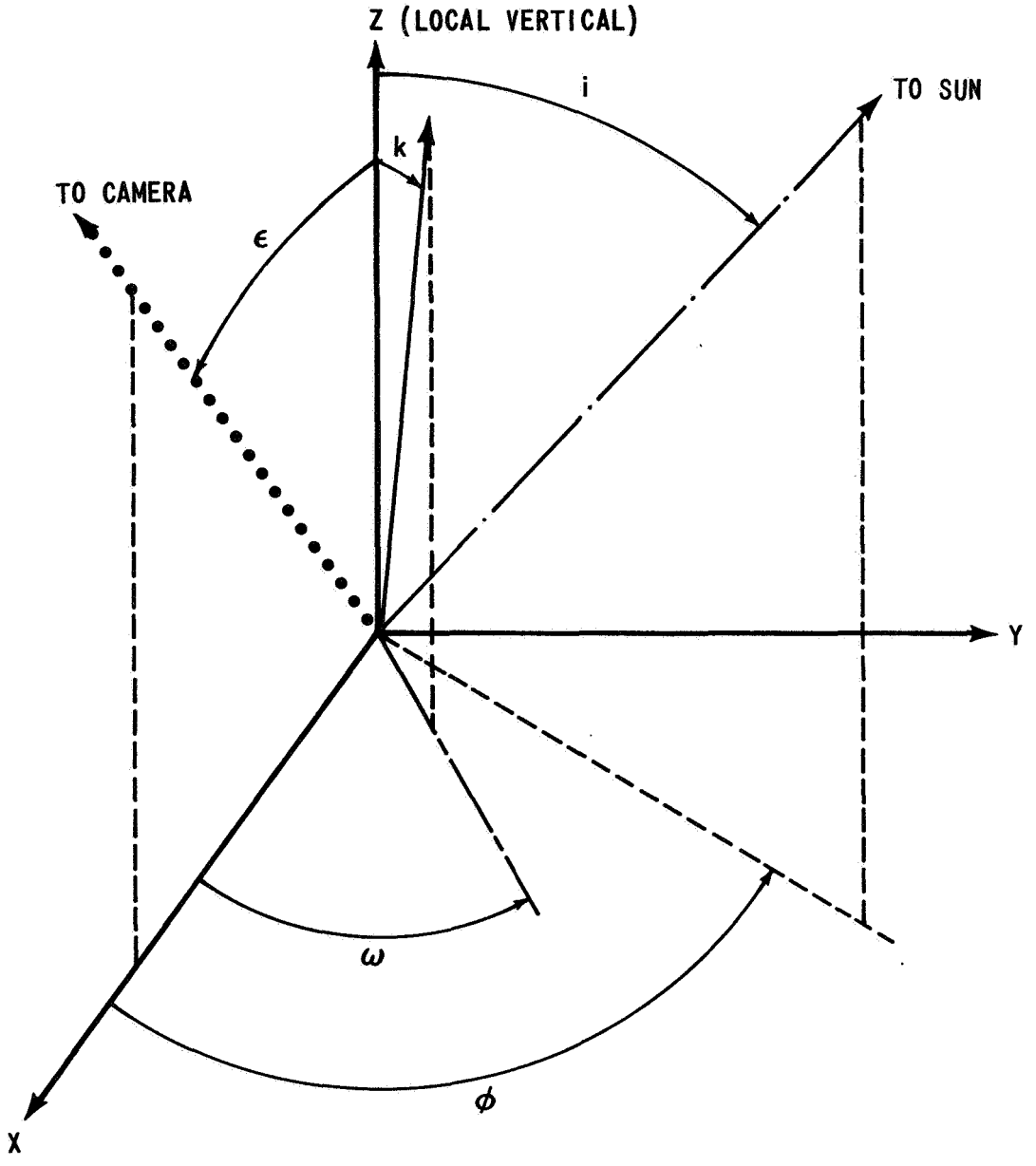

FIGURE 10 - GEOMETRY FOR SLOPE SENSITIVITY

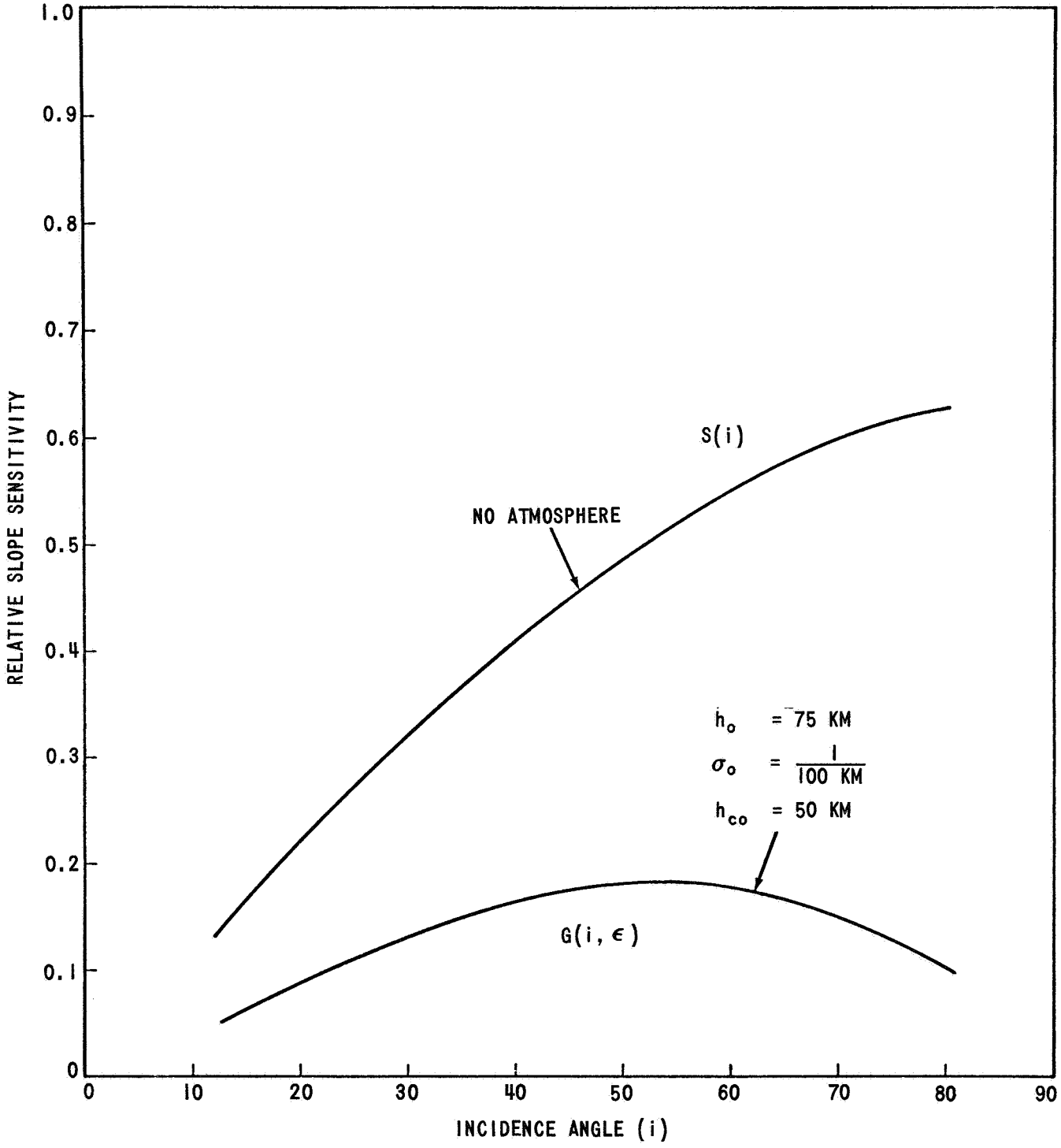

FIGURE 11 - SLOPE SENSITIVITY - LAMBERT SURFACE

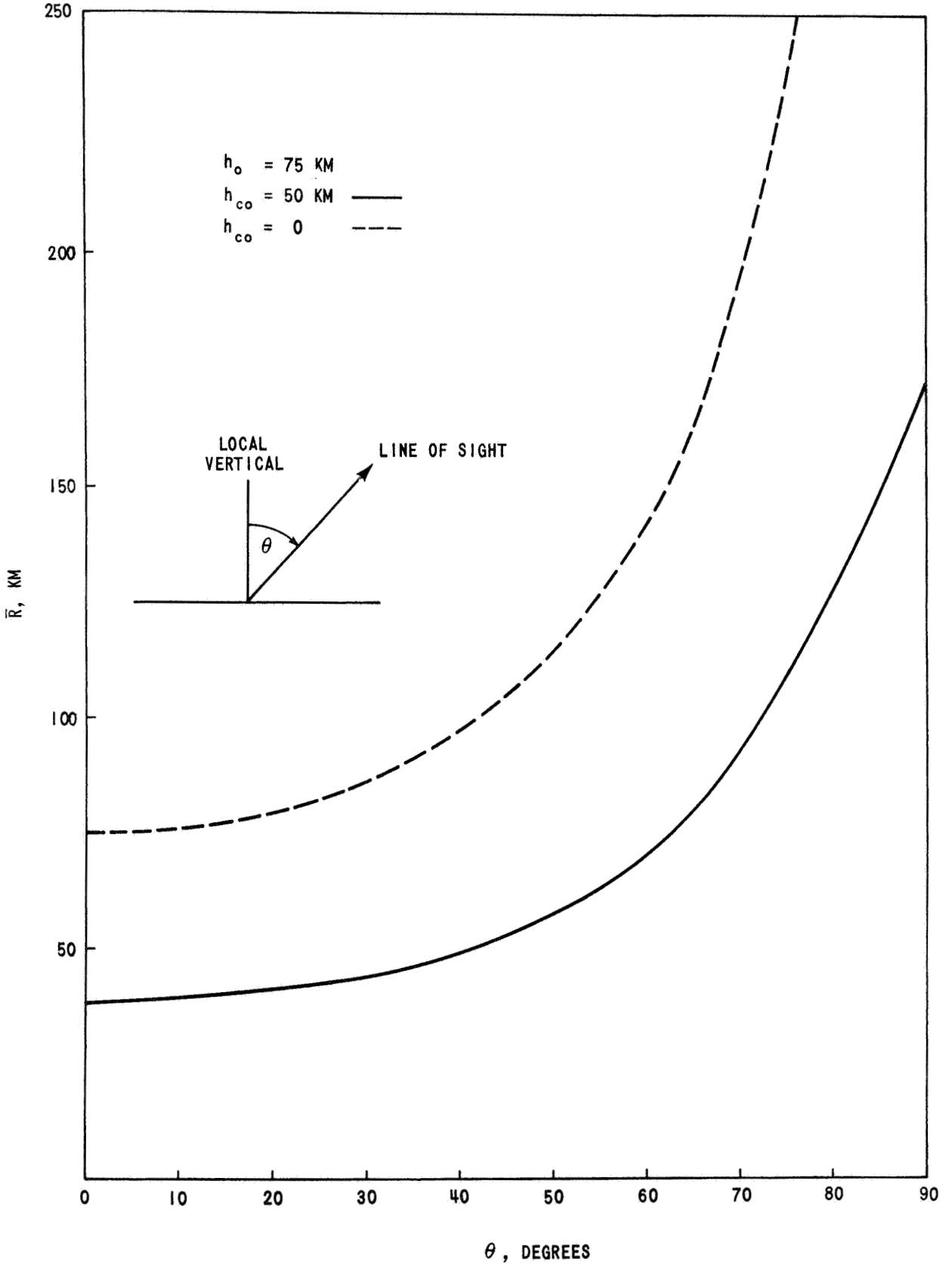

FIGURE 12 - THE QUANTITY $\bar{R}$ AS A FUNCTION OF θ

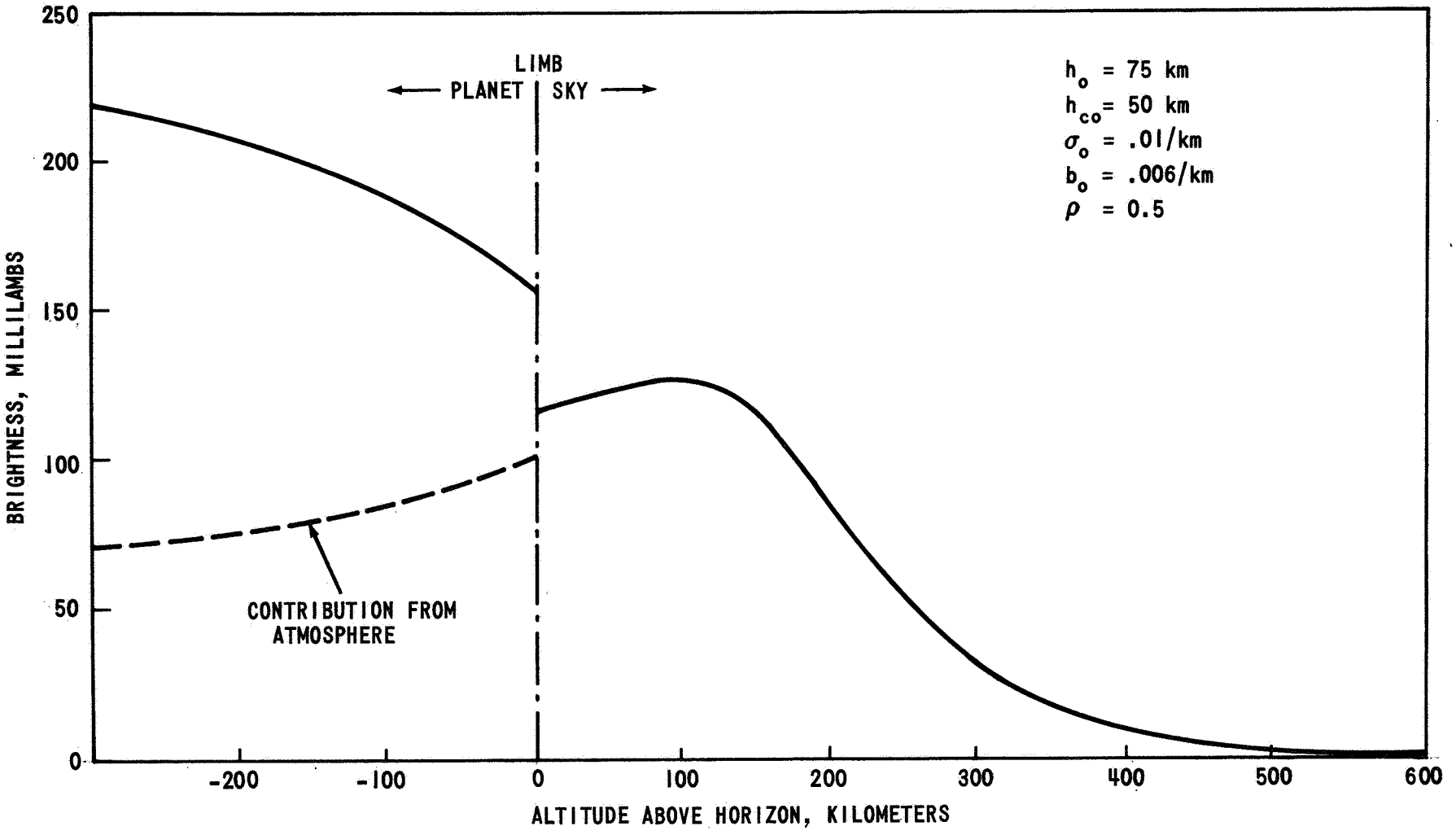

FIGURE 13 - CALCULATED BRIGHTNESS PROFILE FOR MARINER IV PICTURE #1.
THE CONTRIBUTION FROM THE ATMOSPHERE IS THE BRIGHTNESS THAT WOULD BE MEASURED IF THE PLANET SURFACE WERE COMPLETELY BLACK.

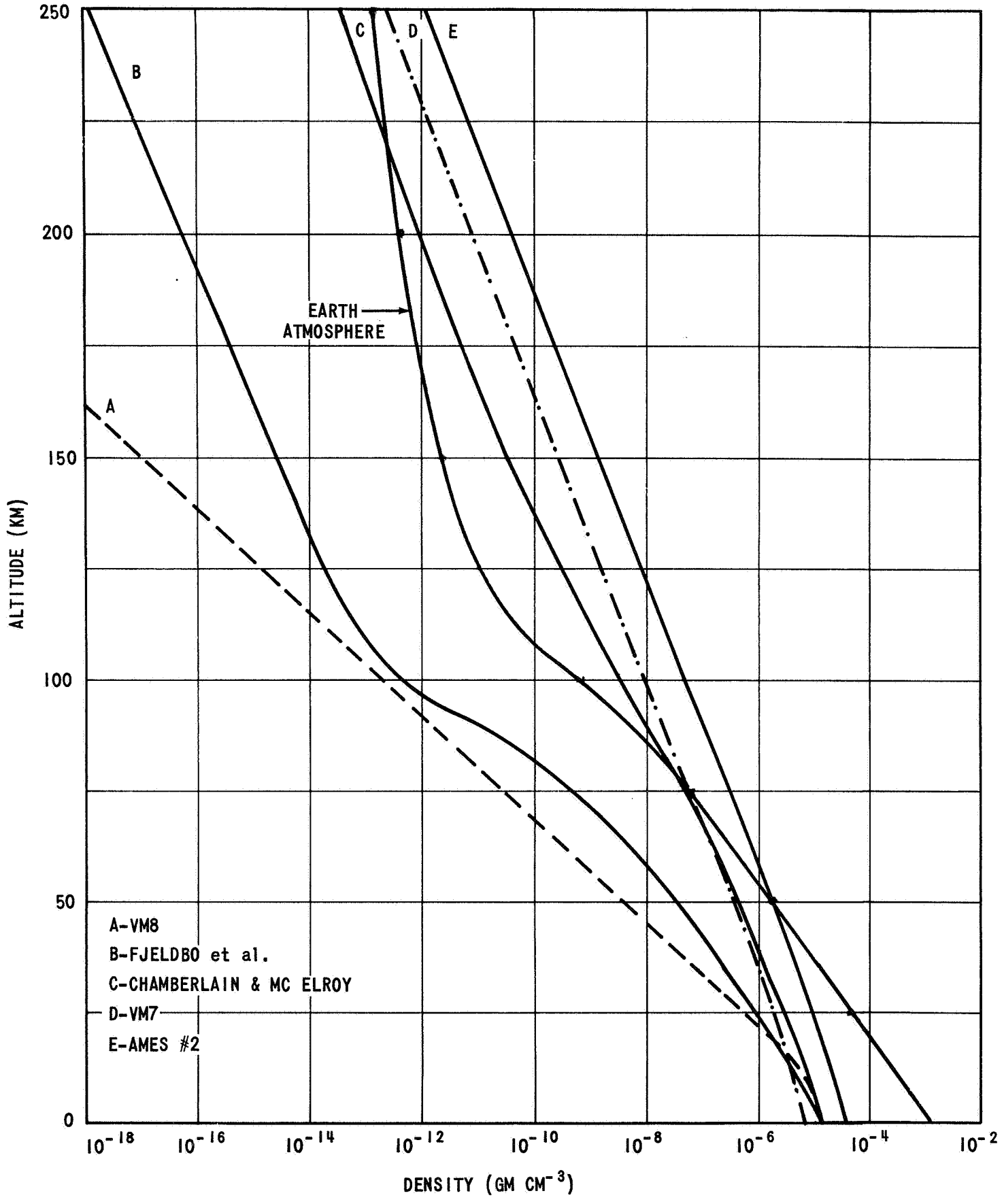

FIGURE 14 - DENSITY PROFILE IN THE EARTH AND MARTIAN ATMOSPHERES

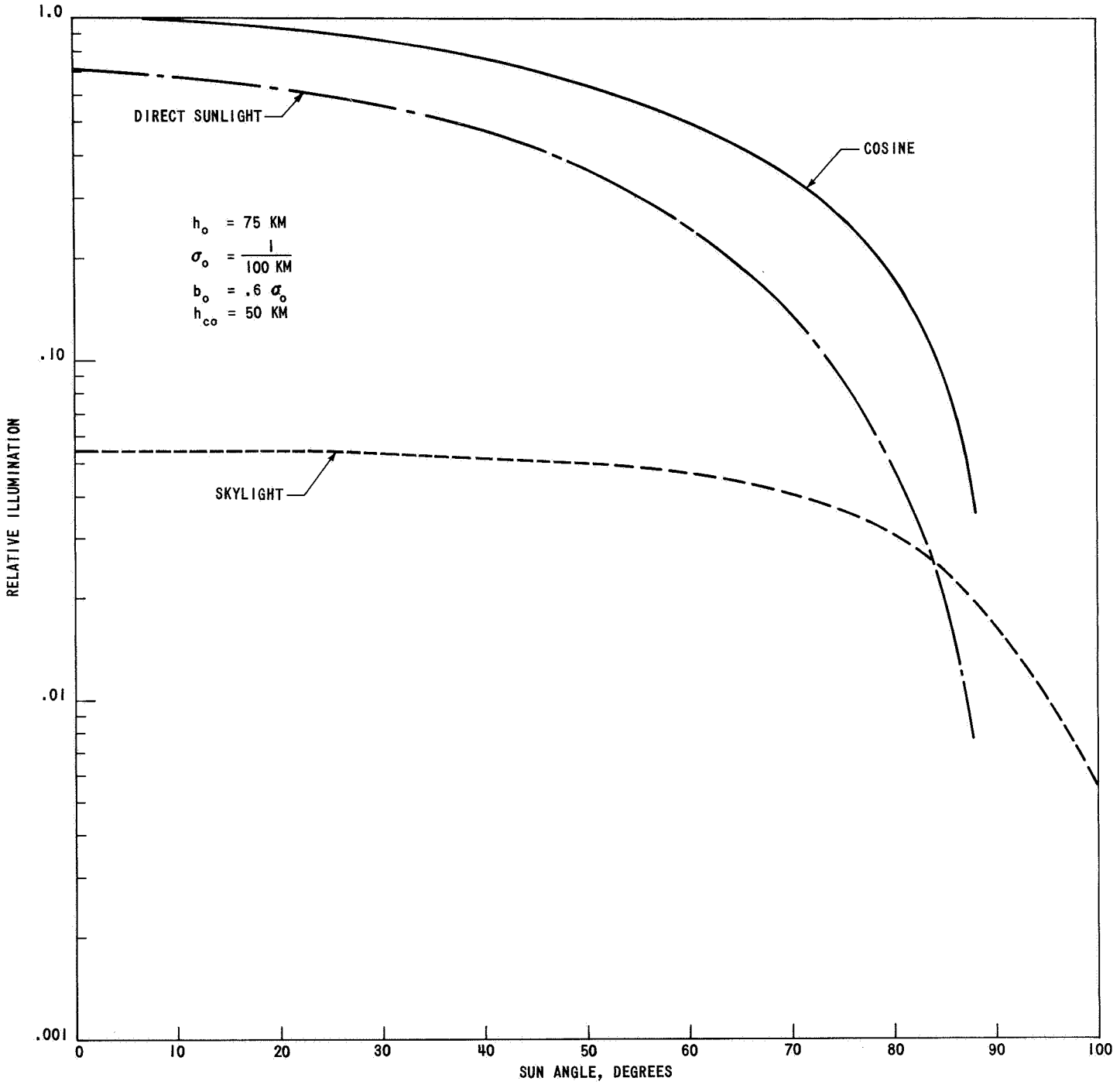

FIGURE 15 - ILLUMINATION OF THE MARTIAN SURFACE REALTIVE TO THE ILLUMINATION OF A SURFACE OUTSIDE THE ATMOSPHERE AND NORMAL TO THE INCIDENT SUNLIGHT. THE COSINE CURVE GIVES THE ILLUMINATION OF THE PLANETARY SURFACE IF THERE IS NO ATMOSPHERE

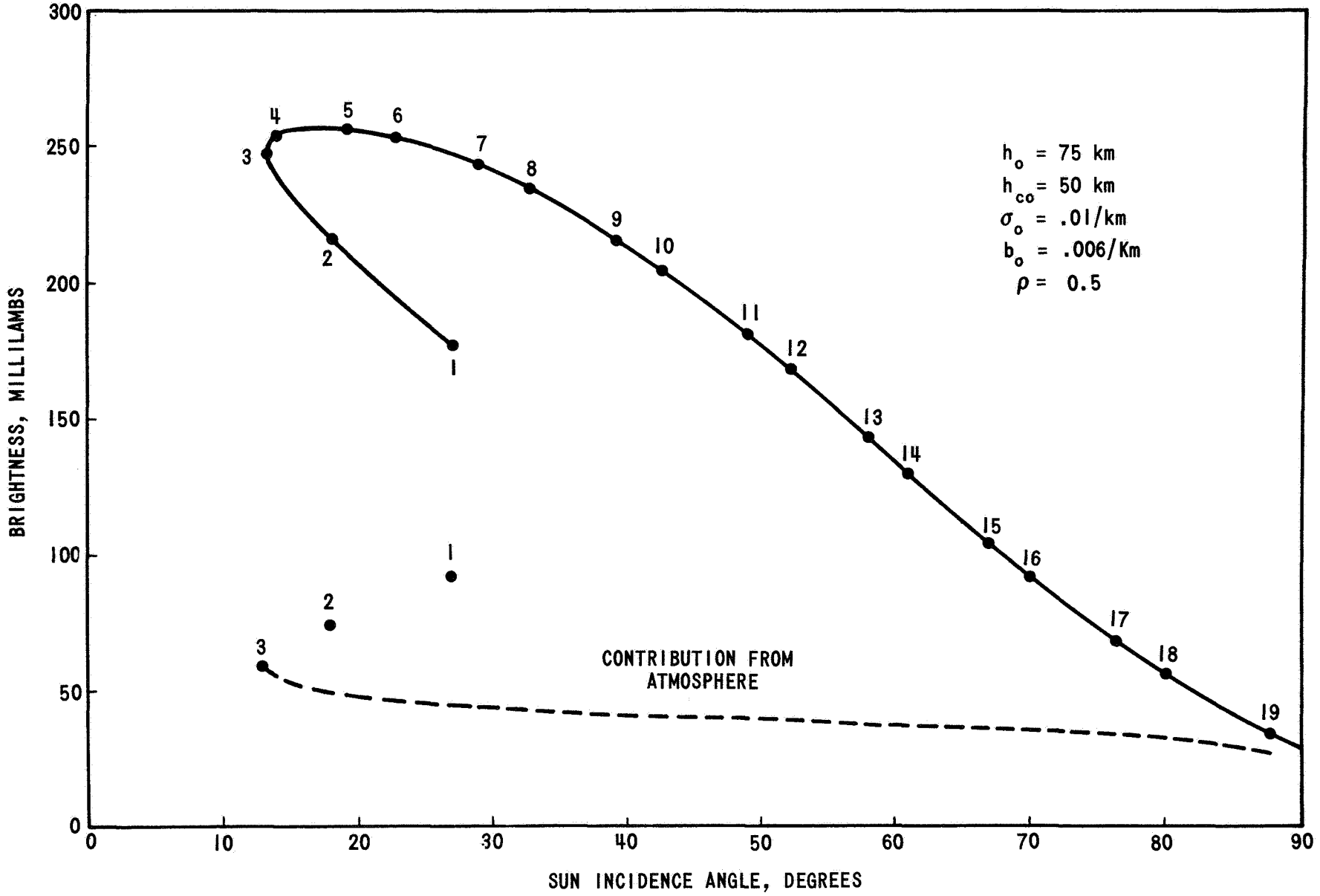

FIGURE 16 - CALCULATED BRIGHTNESS AT THE CENTER OF MARINER IV PICTURES. THE CONTRIBUTION FROM THE ATMOSPHERE IS THE BRIGHTNESS THAT WOULD BE MEASURED IF THE PLANET SURFACE WERE COMPLETELY BLACK.

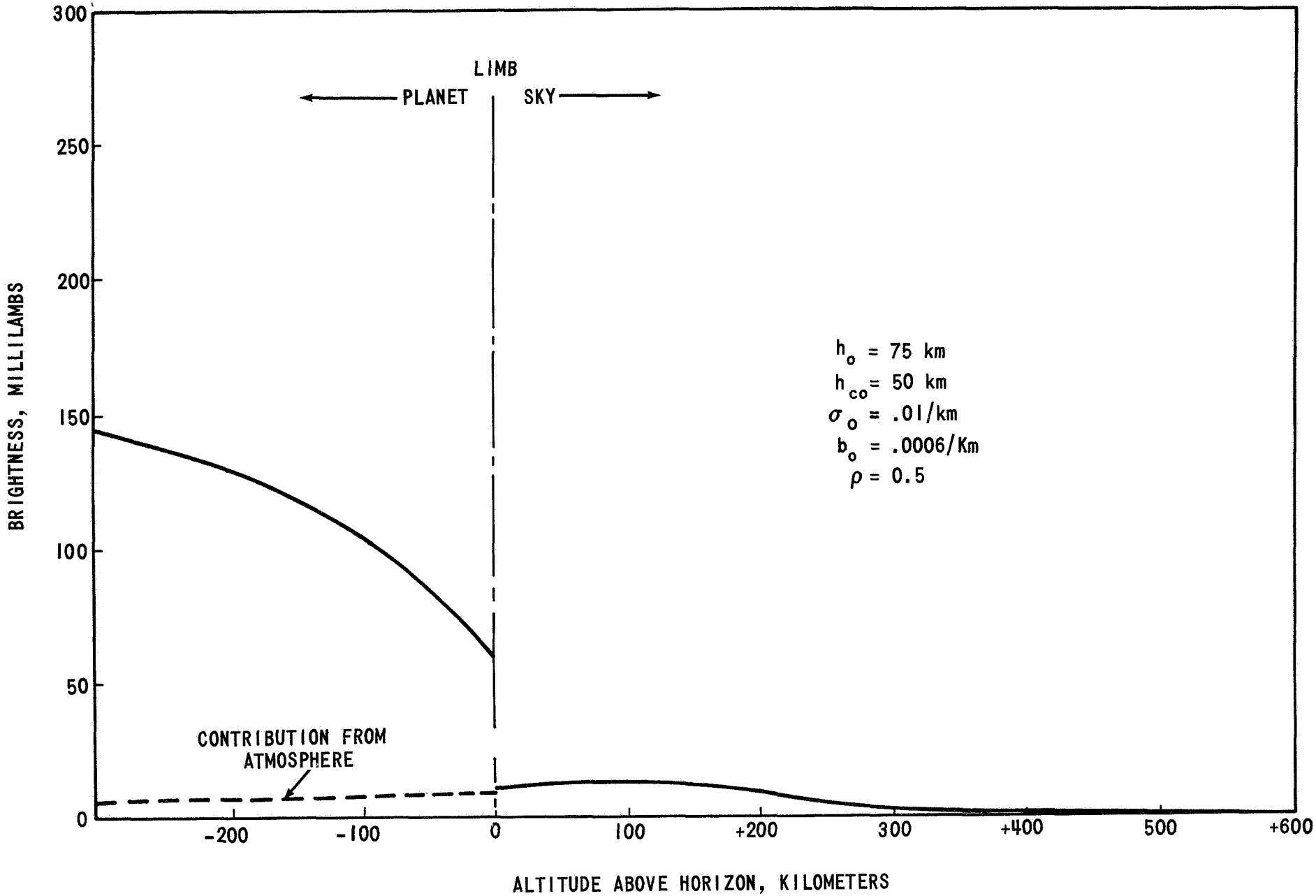

FIGURE 17 - CALCULATED BRIGHTNESS PROFILE FOR MARINER IV PICTURE #1.

THE PARAMETERS WERE CHOSEN UNDER THE ASSUMPTION THAT THE PICTURE CONTAINS A SIGNIFICANT PROPORTION OF GLARE.

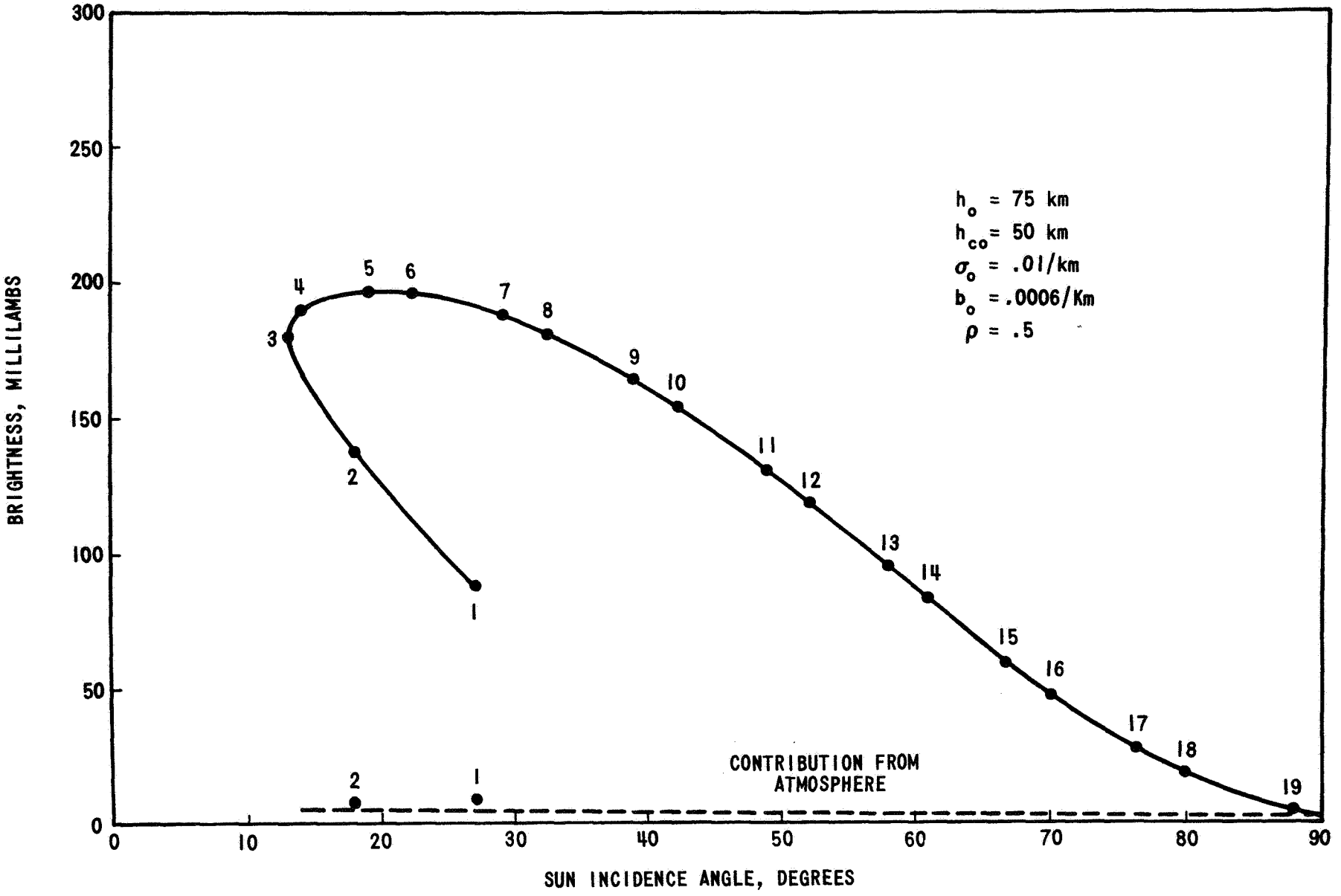

FIGURE 18 - CALCULATED BRIGHTNESS PROFILE AT THE CENTER OF MARINER IV PICTURES. THE PARAMETERS WERE CHOSEN TO FIT THE ASSUMPTION THAT PICTURE #1 CONTAINS A SIGNIFICANT PROPORTION OF GLARE.

BELLCOMM, INC.

DISTRIBUTION LIST

NASA Headquarters
Messrs. R. J. Allenby/MAL
W. P. Armstrong/MTX
W. E. Brunk/SL
R. P. Bryson/MAL
N. W. Cunningham/SL
F. P. Dixon/MTY
S. E. Dwornik/SL
R. F. Fellows/SL
E. W. Glahn/SL
E. W. Hall/MTG
D. P. Hearth/SL
W. Jakobowski, SL
T. A. Keegan/MA-2
R. S. Kraemer/SL
U. Liddel/SS
D. R. Lord/MTD
M. A. Mitz/SL
M. W. Molloy/MAL
D. G. Rea/SL
G. Reiff/SL
A. D. Schnyer/MTV
A. T. Strickland/MAL
J. W. Wild/MTE
V. R. Wilmarth/MAL

Ames Research Center
D. Gault/SSP
L. Roberts/M (2)

California Institute of Technology
D. L. Anderson
N. W. Horowitz
R. B. Leighton
B. C. Murray
R. P. Sharp

Goddard Space Flight Center
I. Adler/641

Jet Propulsion Laboratory
J. D. Allen/323
A. G. Herriman/32
D. Schneiderman/251
H. M. Schurmeier/241
R. K. Sloan/323

Langley Research Center
Messrs. C. Broome/159
J. S. Martin/200
I. Taback/159
T. Young/159

Manned Spacecraft Center
W. N. Hess/TA

Massachusetts Institute of Technology
J. Beckerly
T. McCord
F. Press

Bellcomm Inc.
F. G. Allen
G. M. Anderson
A. P. Boysen, Jr.
D. A. Chisholm
D. A. DeGraaf
J. P. Downs
R. E. Gradle
D. R. Hagner
P. L. Havenstein
N. W. Hinners
B. T. Howard
D. B. James
J. Kranton
H. S. London
K. E. Martersteck
R. K. McFarland
J. Z. Menard
G. T. Orrok
T. L. Powers
I. M. Ross
F. N. Schmidt
W. B. Thompson
C. C. Tiffany
J. W. Timko
J. M. Tschirgi
R. L. Wagner
J. E. Waldo
All members, Division 101
Central Files
Department 1023
Library